Research

Free-matrix-based integral inequalities for sampled-data synchronization control of delayed complex networks

Qinjun Zeng[1,2] · Minghui Jiang[1,2] · Junhao Hu[3]

Received: 20 July 2023 / Accepted: 2 October 2023
Published online: 29 October 2023

Abstract
The issue of synchronizing delayed and complicated dynamical networks (CDNs) using sampling data is examined in this research. First, modified free-matrix-based integral inequalities (MFMBIIs), respectively, are generated from the current free-matrix-based integral inequalities (FMBIIs) [36] and [37] to optimize CDNs' sampled-data synchronizing control's efficiency. Following that, the intended data sampling controller is put forth to asymptotically and exponentially synchronize the CDNs by deploying the time-associated Lyapunov functional technique and convexity-based combining approach, which fully utilize the acceptable information with respect to the actual sampling interval. Finally, computational instances verify the validity of the present outcomes and especially show that a larger upper bound of the sampling interval can be obtained from our results.

Article highlights

- Time-dependent continuous Lyapunov functions are created with sufficient reliable data aboutthe current sampling sequence to lower the restrictiveness of the suggested conclusions.
- Modified free-matrix-based integral inequalities (MFMBIIs) are proposed.
- Numerical examples demonstrate how our findings can be used to get a larger upper constrainton the sampling interval.

Keywords Dynamically complex networks · Sampled-data controlling · Asymptotical synchronization · Exponential synchronization

1 Introduction

Complex dynamic networks (CDNS) have received a lot of attention because they can be used to accurately model a variety of reality-related systems, including global networks, socially relevant networks, power grids, etc [1–3]. In addition, as a major group behavior, synchronization of complex networks has been widely discussed because of its uncertain uses in communication security, biological processes, the formation of harmonic oscillations, and the design of chaos generators. [4–7]. On the other side, some control mechanisms have been put forth to address the

✉ Minghui Jiang, jiangminghui@ctgu.edu.cn; Qinjun Zeng, 3097517851@qq.com; Junhao Hu, junhaohu74@163.com | [1]Three Gorges Mathematical Research Center, China Three Gorges University, Yichang, China. [2]Institute of Nonlinear Complex Systems, China Three Gorges University, Yi Chang 443000, Hubei, China. [3]College of Mathematics and Statistics, South Central University for Nationalities, Wuhan 430074, Hubei, China.

synchronization challenge faced by CDNs, including pinning control [10], adaptive control [9], and impulsive control [8], among others. The above control strategies have continuity. This means that state variables are acquired, sent, and handled every minute, which is sometimes impossible to guarantee in the actual world [11]. Influenced by the rapid development of computers for evaluating and smart devices, continuous-time controls are increasingly being replaced by electronic controls, as the latter might offer higher dependability, accuracy, and stability. As a result, controls that utilize discontinuous data have garnered a lot of interest [12–15]. The sampled-data control method has various benefits over some continuous control approaches, including ease of installation, compact size, cheap maintenance costs, and effectiveness in achieving CDNs synchronization [16]. However, only a few papers have studied the synchronization problem of complex networks in the sense of sampling, such as [3, 4, 16].

Three kinds in particular have emerged from the examination of sampled-data systems. By converting the system over data sampling into a discontinuous system before analyzing it [17–19], the first method called the discrete-time technique is usually used. In the second method, the sampling system is viewed from the viewpoint of a hybrid system, an impulse model is constructed to describe it, and the stability theorem is obtained by employing discontinuous Lyapunov functional analysis [20, 21]. The last input delay method has been developed from a continuous-time perspective, particularly for systems with various delays in time [22, 23]. Researchers have developed and improved a number of methods within this framework, including the looped functioning-based approach [24], the discontinuous Lyapunov functional methodology [25, 26], and the time-dependent Lyapunov functioning technique [27–29]. By constructing a continuous Lyapunov function for neural networks, improved synchronization conditions with control using sampled data were obtained [30]. The constraints derived in [31] are less conservative than [32] because the sawtooth characteristic information about the variable in time delay is captured by the continuous Lyapunov functional. However, the outcomes are still overly conservative even when each integrating variable included in the appropriate Lyapunov functional's derivative is addressed by implementing the Jensen inequality [31]. In an effort to boost the effectiveness of collecting information mastery for synchronizing chaotic Lur'e systems, methods rooted in free matrix inequalities (FMIs) from [33] and [34] in [35] have been implemented more recently. However, from the existing literature [30–35], we can see that there is still room for improvement in Jensen inequality and free matrix inequality methods.

Based on past discussions, we look into the synchronization control issue with discontinuous sampled data for delayed complex networks in this research. The following three significant contributions are highlighted: (1) The use of a data sampling controller for synchronization control in delayed complex networks is discussed. (2) To handle the Lyapunov function's derivative, modified free-matrix-based integral inequalities (MFMBIIs) with less conservatism and lower computational complexity are suggested. To make certain that the error system that occurs from investigating is asymptotically and exponentially stable, respectively, novel requirements are derived. (3) Time-dependent continuous Lyapunov functions are created with sufficient reliable data about the current sampling sequence, which appropriately lowers the restrictiveness of the suggested conclusions. The paper deviates from the previous findings in [2, 4, 7] in that it only allows positive definiteness for each term of the constructed Lyapunov-Krasovskii functions (LKFs). The LKFs are made positive-definite in the current work by taking them into account as a whole.

Notations: $\mathfrak{R}^n$ refers to Euclidean space with n dimensions in this paper. $||\cdot||$ stands for the Euclidean vector norm. The sign $Y > 0$ for any matrix Y suggests that the structure of the matrix is positively defined. $Sym\{Y\}$ is denoted by $Y + Y^T$. The signs $-1$and T, respectively, indicate the inverse as well as the transposition of matrices. Arranged symmetrically, elements in a symmetrical matrix are indicated by the symbol $*$. The Kronecker product is represented with the notation $\otimes$. For a real symmetric matrix $\mathcal{P}$, the maximum of its eigenvalue is denoted by $\lambda_{max}(\mathcal{P})$. $diag\{\cdots\}$ refers to the diagonally blocked matrix. As the identity matrix, $\amalg$ is defined.

2 Preliminaries

Consider the complicated network displayed below, in which a nonlinear dynamic follower system with n dimensions makes up each node and there are $\mathcal{N}$ identically connected nodes in total:

$$\begin{cases} \dot{e}_p(\hat{t}) = \pounds(e_p(\hat{t})) + c\sum\limits_{q=1,q\neq p}^{\mathcal{N}} \mathcal{G}_{pq}\mathcal{A}(e_q(\hat{t}-\ell) - e_p(\hat{t}-\ell)) + u_p(\hat{t}), \\ y_p(\hat{t}) = \eth e_p(\hat{t}), p = 1, 2, \ldots, \mathcal{N}, \end{cases} \tag{1}$$

where the control input and state variable relating to the pth node, respectively, are $u_p(\hat{t})$ and $e_p(\hat{t}) \in \mathfrak{R}^n$. The dynamics of nodes is described by the nonlinear vector-valued function $\pounds(e_p(\hat{t})) = (\pounds_1(e_p(\hat{t})), \pounds_2(e_p(\hat{t})), \ldots, \pounds_n(e_p(\hat{t})))^T \in \mathfrak{R}^n$. The coupling force is suggested with c, and the time delay, ℓ,

is constant. The following outer connecting configuration matrix $\mathscr{G} = (\mathscr{G}_{pq})_{\mathscr{N}\times\mathscr{N}} \in \mathfrak{R}^{\mathscr{N}\times\mathscr{N}}$ is represented as: $\mathscr{G}_{pq} = 0$ when the relation connecting nodes q to $p(p \neq q)$ doesn't exist; in other cases, $\mathscr{G}_{pq} > 0$. The diagonally oriented components of $\mathscr{G}$ are represented with the symbol $\mathscr{G}_{pp} = -c \sum_{q=1,q\neq p}^{\mathscr{N}} \mathscr{G}_{pq}$. The unchanged internal coupling matrix is denoted as $\mathscr{A} = (\mathscr{A}_{pq})^{n\times n} \in \mathfrak{R}^{n\times n}$. $y_p(t)$ refers to the produced measurements associated with the pth node, and the matrix $\mathfrak{O}$ has been identified and has a proper dimension.

Assumption 1 The continual non-linear function $\pounds(\cdot) : \mathfrak{R}^n \to \mathfrak{R}^n$ is a sector valued in addition to meeting the condition as follows:

$$(\pounds(v) - \pounds(w) - S_1(v-w))^T(\pounds(v) - \pounds(w) - S_2(v-w)) \leq 0, \quad \forall v, w \in \mathfrak{R}^n, \tag{2}$$

Consider the controller for data sampling as follows:

$$u_p(\hat{t}) = \daleth_p \hat{e}_p(\hat{t}_f),\ \hat{t}_f \leq \hat{t} < \hat{t}_{f+1}, p = 1, 2, \ldots, \mathscr{N}, \tag{4}$$

from which the controlling gain matrix needs to be built, which is $\daleth_p \in \mathfrak{R}^{n\times n}$.

The synchronization error system (ES) is then displayed with the following structure:

$$\begin{cases} \dot{\hat{e}}_p(\hat{t}) = \pounds(e_p(\hat{t})) - \pounds(\curlywedge(\hat{t})) + c\sum_{q=1}^{\mathscr{N}} \mathscr{G}_{pq}\mathscr{A}\hat{e}_q(\hat{t}-\ell) + \daleth_p\hat{e}_p(\hat{t}_f), \\ \hat{y}_p(\hat{t}) = \mathfrak{O}e_p(\hat{t}) - \mathfrak{O}\curlywedge(\hat{t}) = \mathfrak{O}\hat{e}_p(\hat{t}),\ \hat{t}_f \leq \hat{t} < \hat{t}_{f+1}, \end{cases} \tag{5}$$

and Eq. (5) could be established as

$$\begin{cases} \dot{\hat{e}}(\hat{t}) = \beth(\hat{e}(\hat{t})) + c(\mathscr{G}\otimes\mathscr{A})\hat{e}(\hat{t}-\ell) + \daleth\hat{e}(\hat{t}_f), \\ \hat{y}(\hat{t}) = (I_{\mathscr{N}}\otimes\mathfrak{O})\hat{e}(\hat{t}),\ \hat{t}_f \leq \hat{t} < \hat{t}_{f+1}, \end{cases} \tag{6}$$

in which

$\hat{y}(\hat{t}) = (\hat{y}_1^T(\hat{t}), \hat{y}_2^T(\hat{t}), \ldots, \hat{y}_{\mathscr{N}}^T(\hat{t}))^T$, $\hat{e}(\hat{t}) = (\hat{e}_1^T(\hat{t}), \hat{e}_2^T(\hat{t}), \ldots, \hat{e}_{\mathscr{N}}^T(\hat{t}))^T$, $\daleth = diag\{\daleth_1, \daleth_2, \cdots, \daleth_{\mathscr{N}}\}$,
$\beth(\hat{e}(\hat{t})) = (\beth^T(e_1(\hat{t})) - \beth^T(\curlywedge(\hat{t})), \beth^T(e_2(\hat{t})) - \beth^T(\curlywedge(\hat{t})), \ldots, \beth^T(e_{\mathscr{M}}(\hat{t})) - \beth^T(\curlywedge(\hat{t})))^T$.

where S_1 and S_2 denote recognized constant matrices and have the required dimensions.

Therefore, the representation of the synchronization error is

$$\hat{e}_p(\hat{t}) = e_p(\hat{t}) - \curlywedge(\hat{t}), p = 1, 2, \ldots, \mathscr{N},$$

in which, known as the leader node, the state evolution of the unrestrained isolation node is denoted as $\curlywedge(\hat{t}) \in \mathfrak{R}^n$ and fulfills:

$$\dot{\curlywedge}(\hat{t}) = \pounds(\curlywedge(\hat{t})). \tag{3}$$

Assumption 2 The discontinuous measurements associated with $e(\hat{t})$ and $\curlywedge(\hat{t})$ during the sampling moment $\hat{t}_f$, respectively, are denoted by $e(\hat{t}_f)$ and $\curlywedge(\hat{t}_f)$ and are accessible, and a holder of zero orders yields and outputs the control signal at a string of hold intervals,

$$0 = \hat{t}_0 < \hat{t}_1 < \cdots < \hat{t}_f < \cdots < \lim_{f\to\infty} \hat{t}_f = +\infty,$$

where

$$\hat{t}_{f+1} - \hat{t}_f = d_f \in (0, d].$$

d_f stands for sampling periods for all $f \geq 0$, while d stands for the upper limit of sampling intervals.

Throughout this research, the synchronization of the $\mathscr{N}$ follower systems (FSs) (1) and the leader system (LS) (3) is respected to be acquired by using the controller (4) with sampling data. In essence, the associated status trajectory of ES (6) gets closer to the origin in a gradual or exponential manner for any initial condition.

Proposition 1 *ES (6) is assumed to be asymptotically stable. If for any started situation* $\hat{e}(\hat{t}_0)$,

$$\lim_{\hat{t}\to+\infty} ||\hat{e}(\hat{t})|| = 0.$$

Proposition 2 *It is assumed that ES (6) is exponentially stable. If given a pair of constants,* $\mathfrak{z} > 0$ *and* $\mathfrak{d} > 0$,

$$||\hat{e}(\hat{t})|| \leq \mathfrak{d}e^{-\mathfrak{z}\hat{t}} \sup_{-\ell\leq j\leq 0} \left\{||\hat{e}(j)||, ||\dot{\hat{e}}(j)||\right\}$$

for any starting condition $\hat{e}(\hat{t}_0)$, *where* $\mathfrak{d}$ *and* $\mathfrak{z}$ *are present, respectively, as the decaying coefficient and decaying rate.*

Lemma 1 (Zeng, He, Wu, and She [33]). *Assuming that the function e is differential and defined on*: $[\ltimes, \veebar] \to \mathfrak{R}^n$. *The following inequality is true with regard to symmetry matrices* $\mathscr{R} \in \mathfrak{R}^{n\times n}, U_1, U_3 \in \mathfrak{R}^{3n\times 3n}$, *as well as whatever matrices* $U_2 \in \mathfrak{R}^{3n\times 3n}, M_1, M_2 \in \mathfrak{R}^{3n\times n}$ *fulfill*

$$\bar{\Phi}=\begin{bmatrix} U_1 & U_2 & M_1 \\ * & U_3 & M_2 \\ * & * & \mathscr{R} \end{bmatrix}\geq 0:$$
$$-\int_{\ltimes}^{\veebar}\dot{e}^T(\wp)\mathscr{R}\dot{e}(\wp)d\wp\leq\phi^T(\ltimes,\veebar)\Psi(\ltimes,\veebar)\phi(\ltimes,\veebar),$$

where

$$\Psi(\ltimes,\veebar)=(\veebar-\ltimes)\Big(U_1+\frac{1}{3}U_3\Big)+Sym\{M_1\bar{\Phi}_1+M_2\bar{\Phi}_2\},$$
$$\bar{\Phi}_1=\flat_1-\flat_2,\ \bar{\Phi}_2=2\flat_3-\flat_1-\flat_2,$$
$$\flat_1=[\amalg\ 0\ 0],\flat_2=[0\ \amalg\ 0],\flat_3=[0\ 0\ \amalg],\phi(\ltimes,\veebar)$$
$$=\left[e^T(\veebar)\ e^T(\ltimes)\ \frac{1}{\veebar-\ltimes}\int_{\ltimes}^{\veebar}e^T(\wp)d\wp\right]^T.$$

Lemma 2 (Lee and Park [36]). *Assuming the function e is a differentiable function and defined on*: $[\ltimes,\veebar]\to\mathfrak{R}^n$. *With regard to a symmetry matrix* $\mathscr{R}\in\mathfrak{R}^{n\times n}>0$, *as well as whatever matrices* $M_1,M_2\in\mathfrak{R}^{3n\times n}$, *the inequality is true as follows*:

$$-\int_{\ltimes}^{\veebar}\dot{e}^T(\wp)\mathscr{R}\dot{e}(\wp)d\wp\leq\varpi^T(\ltimes,\veebar)\Psi(\ltimes,\veebar)\varpi(\ltimes,\veebar),$$

where

$$\varpi(\ltimes,\veebar)=\left[e^T(\veebar)\ e^T(\ltimes)\int_{\ltimes}^{\veebar}e^T(\wp)d\wp\right]^T,$$
$$\Psi(\ltimes,\veebar)=(\veebar-\ltimes)\Big(P_1+\frac{(\veebar-\ltimes)^2}{3}P_2-Sym\{[M_2\ M_2\ 0]\}\Big)$$
$$+Sym\{[M_1\ -M_1\ 2M_2]\},$$
$$P_1=M_1\mathscr{R}^{-1}{M_1}^T,P_2=M_2\mathscr{R}^{-1}{M_2}^T.$$

Remark 1 The primary distinction in Lemma 2 is that $\frac{1}{\veebar-\ltimes}\int_{\ltimes}^{\veebar}e(\wp)d\wp$ is replaced by $\int_{\ltimes}^{\veebar}e(\wp)d\wp$ in an augmented vector $\varpi(\ltimes,\veebar)$. For sampled-data systems, this characteristic is advantageous. Allow $\varpi(\ltimes,\veebar)=\frac{1}{\veebar-\ltimes}\int_{\ltimes}^{\veebar}e(\wp)d\wp$ to be the value. The phrase $\int_{\hat{t}-\varsigma(\hat{t})}^{\hat{t}}e(\wp)d\wp=\varsigma(\hat{t})\varpi(\hat{t}-\varsigma(\hat{t}),\hat{t})$ is required to be included within the expanded vector of stabilized requirements when Lemma 1 is implemented in the time-dependent delaying system, and it might be dealt with using the convex combinating method. The term "$(\hat{t}-\hat{t}_f)\varpi(\hat{t}_f,\hat{t})$", however, creates a challenge when it comes to systems with sampling data since the convex combination approach couldn't be used to handle the term, $\hat{t}-\hat{t}_f$, as for the discrete property of the systems with sampling data, i.e., $\hat{t}-\hat{t}_f\in[0,d)$ for $\hat{t}\in[\hat{t}_f,\hat{t}_{f+1})$. Due to this issue, it was determined that the most widely used inequalities were unable to serve as a tool for data sampling systems with time delays; nevertheless, the MFMBII presented in Lemma 2 could be used in this situation. Lemma 1 uses $24.5n^2+3.5n$ various deciding factors; however, Lemma 2 adopts $6.5n^2+0.5n$, which is an additional benefit. In other words, Lemma 2 can significantly simplify the stability criteria's numerical complexity.

Remark 2 It should be noted that the numerical factor of the matrix P_2 in Lemma 2, $\frac{(\veebar-\ltimes)^2}{3}$, is expected to be $\frac{d^2}{3}$ to adopt the convex combination approach in the sampling system, where d is an upper limit on the sample period of the system. This truth causes conservatism in our findings, so we suggest the next lemma to fix this problem. Compared with the existing results [33, 36], the inequality proposed in Lemma 3 deserves to be widely applied to sampled-data systems since it is less conservative and computationally complex in deriving treatable stability conditions expressed in terms of linear matrix inequalities.

Lemma 3 *Assuming the function e is a differentiable function and defined on*: $[\ltimes,\veebar]\to\mathfrak{R}^n$. *In relation to a symmetry matrix* $\mathscr{R}\in\mathfrak{R}^{n\times n}>0$, whatever matrices $M_1,M_2\in\mathfrak{R}^{3n\times n}$, *the inequality is true as follows*:

$$-\int_{\ltimes}^{\veebar}\dot{e}^T(\wp)\mathscr{R}\dot{e}(\wp)d\wp\leq\varpi^T(\ltimes,\veebar)\Psi(\ltimes,\veebar)\varpi(\ltimes,\veebar),$$

where

$$\varpi(\ltimes,\veebar)=\left[e^T(\veebar)\ e^T(\ltimes)\int_{\ltimes}^{\veebar}e^T(\wp)d\wp\right]^T,$$
$$\Psi(\ltimes,\veebar)=(\veebar-\ltimes)\Big(P_1+\frac{1}{3}P_2\Big)$$
$$+Sym\{M_1(\flat_1-\flat_2)+M_2(2\flat_3-\flat_1-\flat_2)\},$$
$$\flat_1=[\amalg\ 0\ 0],\flat_2=[0\ \amalg\ 0],\flat_3=[0\ 0\ \amalg],$$
$$P_1=M_1\mathscr{R}^{-1}{M_1}^T,P_2=M_2\mathscr{R}^{-1}{M_2}^T.$$

Proof The following inequality holds according to the fact that $\mathscr{R}>0$ and Schur complement:

$$\begin{bmatrix} M_1\mathscr{R}^{-1}M_1^T & M_1\mathscr{R}^{-1}M_2^T & M_1 \\ * & M_2\mathscr{R}^{-1}M_2^T & M_2 \\ * & * & \mathscr{R} \end{bmatrix}\geq 0.$$

By replacing $\phi(\ltimes, \veebar)$ with $\varpi(\ltimes, \veebar)$ and $U_1 = M_1\mathscr{R}^{-1}M_1^T$, $U_2 = M_1\mathscr{R}^{-1}M_2^T$, and $U_3 = M_2\mathscr{R}^{-1}M_2^T$, Lemma 3 could be naturally established employing the same proof strategy as Lemma 1 deployed. □

Lemma 4 (Gunasekaran, Zhai, and Yu [37]). *For matrix* $\mho \in \Re^{3n\times 3n}$ *and positive definite matrix* $\mathcal{Q} \in \Re^{n\times n}$ *fulfilling*

$$\mho = \begin{bmatrix} \mho_{11} & \mho_{12} & \mho_{13} \\ * & \mho_{22} & \mho_{23} \\ * & * & \mho_{33} \end{bmatrix} \geq 0, \mho_{pq} \in \Re^{n\times n}, p, q = 1, 2, 3,$$

and $\mathcal{Q} - \mho_{33} > 0$, *the integral inequality as follows is true*:

$$-\ell \int_{\hat{t}-\ell}^{\hat{t}} \dot{\lambda}^T(\wp)\mathcal{Q}\dot{\lambda}(\wp)d\wp \leq \begin{bmatrix} \lambda(\hat{t}) \\ \lambda(\hat{t}-\ell) \end{bmatrix}^T \begin{bmatrix} H_{11} & H_{12} \\ * & H_{22} \end{bmatrix} \begin{bmatrix} \lambda(\hat{t}) \\ \lambda(\hat{t}-\ell) \end{bmatrix},$$

where

$$H_{11} = -\mathcal{Q} + \mho_{33} + \ell(\ell\mho_{11} + \mho_{13}^T + \mho_{13}),$$
$$H_{12} = \mathcal{Q} - \mho_{33} + \ell(\ell\mho_{12} - \mho_{13} + \mho_{23}^T),$$
$$H_{22} = -\mathcal{Q} + \mho_{33} + \ell(\ell\mho_{22} - \mho_{23} - \mho_{23}^T).$$

$$-\int_0^1 cos(s)3cos(s)ds \leq \begin{bmatrix} 0 & sin(1) \\ & \int_0^1 sin(s)ds \end{bmatrix},$$

Remark 3 Observe that the integral inequality's matrix, $\mathcal{Q}$, in Lemma 4 has a size relationship with the matrix, $\mho_{33}$, with the result that $\mathcal{Q} - \mho_{33} > 0$. In contrast to Lemma 4, Shur complement lemma is utilized to create a matrix in the following lemma, $\mathscr{U}_{12}\mathscr{U}_{22}^{-1}\mathscr{U}_{12}^T$, such that $\mathscr{U}_{11} - \mathscr{U}_{12}\mathscr{U}_{22}^{-1}\mathscr{U}_{12}^T \geq 0$. This makes the matrix in the integral inequality a member of the free matrix. As a result, our findings are substantially shorter. Lemma 4, on the other hand, employs $10n^2$ various deciding factors. The following lemma greatly reduces the numerical complexity of the stability criteria by using $4n^2$ choice variables. Note that the integral inequality method in Lemma 5 was first proposed in [41], then developed and applied to multi-agent networks [37]. Therefore, Lemma 5 provides more useful information about state vectors than Jensen inequality.

Lemma 5 *For a symmetric matrix* $\mathscr{U} \in \Re^{2n\times 2n}$ *satisfying*

$$\mathscr{U} = \begin{bmatrix} \mathscr{U}_{11} & \mathscr{U}_{12} \\ * & \mathscr{U}_{22} \end{bmatrix} \geq 0, \mathscr{U}_{pq} \in \Re^{n\times n}, p, q = 1, 2,$$

the integral inequality displayed below is reliable:

$$-(\hat{t}-\hat{t}_f)\int_{\hat{t}_f}^{\hat{t}} \dot{\lambda}^T(\wp)\mathscr{U}_{11}\dot{\lambda}(\wp)d\wp \leq \begin{bmatrix} \lambda(\hat{t}) \\ \lambda(\hat{t}_f) \end{bmatrix}^T \begin{bmatrix} H_{11} & H_{12} \\ * & H_{22} \end{bmatrix} \begin{bmatrix} \lambda(\hat{t}) \\ \lambda(\hat{t}_f) \end{bmatrix}, \tag{7}$$

where

$$H_{11} = \mathscr{U}_{12}\mathscr{U}_{22}^{-1}\mathscr{U}_{12}^T - \mathscr{U}_{11} + (\hat{t}-\hat{t}_f)^2\mathscr{U}_{22} + 2(\hat{t}-\hat{t}_f)\mathscr{U}_{12},$$
$$H_{12} = -\mathscr{U}_{12}\mathscr{U}_{22}^{-1}\mathscr{U}_{12}^T + \mathscr{U}_{11} - (\hat{t}-\hat{t}_f)\mathscr{U}_{12}^T,$$
$$H_{22} = \mathscr{U}_{12}\mathscr{U}_{22}^{-1}\mathscr{U}_{12}^T - \mathscr{U}_{11}.$$

Proof Think about the following equation:

$$-(\hat{t}-\hat{t}_f)\int_{\hat{t}_f}^{\hat{t}} \dot{\lambda}^T(\wp)\mathscr{U}_{11}\dot{\lambda}(\wp)d\wp$$
$$= -(\hat{t}-\hat{t}_f)\int_{\hat{t}_f}^{\hat{t}} \dot{\lambda}^T(\wp)(\mathscr{U}_{11} - \mathscr{U}_{12}\mathscr{U}_{22}^{-1}\mathscr{U}_{12}^T)\dot{\lambda}(\wp)d\wp \tag{8}$$
$$-(\hat{t}-\hat{t}_f)\int_{\hat{t}_f}^{\hat{t}} \dot{\lambda}^T(\wp)\mathscr{U}_{12}\mathscr{U}_{22}^{-1}\mathscr{U}_{12}^T\dot{\lambda}(\wp)d\wp.$$

By Schur complement, the following is true:

$$\mathscr{U}_{11} - \mathscr{U}_{12}\mathscr{U}_{22}^{-1}\mathscr{U}_{12}^T \geq 0.$$

Therefore,

$$-(\hat{t}-\hat{t}_f)\int_{\hat{t}_f}^{\hat{t}} \dot{\lambda}^T(\wp)(\mathscr{U}_{11} - \mathscr{U}_{12}\mathscr{U}_{22}^{-1}\mathscr{U}_{12}^T)\dot{\lambda}(\wp)d\wp$$
$$\leq -\begin{bmatrix} \lambda(\hat{t}) \\ \lambda(\hat{t}_f) \end{bmatrix}^T \begin{bmatrix} \mathscr{U}_{11} - \mathscr{U}_{12}\mathscr{U}_{22}^{-1}\mathscr{U}_{12}^T & -\mathscr{U}_{11} + \mathscr{U}_{12}\mathscr{U}_{22}^{-1}\mathscr{U}_{12}^T \\ * & \mathscr{U}_{11} - \mathscr{U}_{12}\mathscr{U}_{22}^{-1}\mathscr{U}_{12}^T \end{bmatrix} \begin{bmatrix} \lambda(\hat{t}) \\ \lambda(\hat{t}_f) \end{bmatrix}, \tag{9}$$

where Jensen inequality is applied.

In addition to that,

$$-(\hat{t}-\hat{t}_f)\int_{\hat{t}_f}^{\hat{t}} \begin{bmatrix} \dot{\lambda}(\wp) \\ \lambda(\hat{t}) \end{bmatrix}^T \begin{bmatrix} \mathscr{U}_{12}\mathscr{U}_{22}^{-1}\mathscr{U}_{12}^T & \mathscr{U}_{12} \\ * & \mathscr{U}_{22} \end{bmatrix} \begin{bmatrix} \dot{\lambda}(\wp) \\ \lambda(\hat{t}) \end{bmatrix} d\wp$$
$$= -(\hat{t}-\hat{t}_f)\int_{\hat{t}_f}^{\hat{t}} \dot{\lambda}^T(\wp)\mathscr{U}_{12}\mathscr{U}_{22}^{-1}\mathscr{U}_{12}^T\dot{\lambda}(\wp)d\wp$$
$$-2(\hat{t}-\hat{t}_f)(\lambda^T(\hat{t}) - \lambda^T(\hat{t}_f))\mathscr{U}_{12}\lambda(\hat{t})$$
$$-(\hat{t}-\hat{t}_f)^2\lambda^T(\hat{t})\mathscr{U}_{22}\lambda(\hat{t}).$$

Note that the following is accurate according to Schur complement:

$$\begin{bmatrix} \mathscr{U}_{12}\mathscr{U}_{22}^{-1}\mathscr{U}_{12}^{T} & \mathscr{U}_{12} \\ * & \mathscr{U}_{22} \end{bmatrix} \geq 0.$$

Hence,

$$\begin{aligned} &-(\hat{t}-\hat{t}_f)\int_{\hat{t}_f}^{\hat{t}} \dot{\varkappa}^T(\wp)\mathscr{U}_{12}\mathscr{U}_{22}^{-1}\mathscr{U}_{12}^{T}\dot{\varkappa}(\wp)d\wp \\ &\leq 2(\hat{t}-\hat{t}_f)(\varkappa^T(\hat{t})-\varkappa^T(\hat{t}_f))\mathscr{U}_{12}\varkappa(\hat{t})+(\hat{t}-\hat{t}_f)^2\varkappa^T(\hat{t})\mathscr{U}_{22}\varkappa(\hat{t}) \\ &=\begin{bmatrix} \varkappa(\hat{t}) \\ \varkappa(\hat{t}_f) \end{bmatrix}^T \begin{bmatrix} (\hat{t}-\hat{t}_f)^2\mathscr{U}_{22}+2(\hat{t}-\hat{t}_f)\mathscr{U}_{12} & -(\hat{t}-\hat{t}_f)\mathscr{U}_{12}^{T} \\ * & 0 \end{bmatrix} \begin{bmatrix} \varkappa(\hat{t}) \\ \varkappa(\hat{t}_f) \end{bmatrix}. \end{aligned} \tag{10}$$

Then, Eq. (7) can be derived from (8), (9), and (10). □

3 Sampled-data asymptotical synchronization analysis

The asymptotic synchronization of sampling between FSs (1) and LS (3) is examined in this chapter, and a sufficient condition is discovered.

Regarding brevity, a handful of necessary notations for vectors and matrices have been added,

$$\begin{aligned} &u_1(\hat{t})=\hat{e}(\hat{t})-\hat{e}(\hat{t}_f), u_2(\hat{t})=\hat{e}(\hat{t})-\hat{e}(\hat{t}_{f+1}), \\ &\xi_1(\hat{t})=col\{\hat{e}(\hat{t}_f),\hat{e}(\hat{t}_{f+1})\}, \xi_2(\hat{t})=col\{u_1(\hat{t}),u_2(\hat{t})\}, \\ &\xi_3(\hat{t})=col\{(\hat{t}_{f+1}-\hat{t})u_1(\hat{t}),(\hat{t}-\hat{t}_f)u_2(\hat{t})\}, \\ &w_1(\hat{t})=\int_{\hat{t}_f}^{\hat{t}}\hat{e}(\wp)d\wp, w_2(\hat{t})=\int_{\hat{t}}^{\hat{t}_{f+1}}\hat{e}(\wp)d\wp, \\ &\xi(\hat{t})=col\{\hat{e}(\hat{t}),\hat{e}(\hat{t}_f),\hat{e}(\hat{t}_{f+1}),w_1(\hat{t}),w_2(\hat{t}),\mathfrak{Z}(\hat{e}(\hat{t})),\hat{e}(\hat{t}-\ell),\dot{\hat{e}}(\hat{t})\}, \\ &e_q=\begin{bmatrix} 0_{n\times(q-1)n} & \amalg_n & 0_{n\times(8-q)n} \end{bmatrix}, q=1,2,\ldots,8. \end{aligned}$$

Theorem 1 *For given positive constants* d,ℓ,ρ,γ, *when positive definite and symmetric matrices* $\mathscr{W}_1>0,\mathscr{W}_2>0,\mathscr{P}>0,\mathscr{R}_1>0,\mathscr{R}_2>0$, matrices $\mathscr{Q}_1,\mathscr{Q}_2,M_1,M_2,N_1,N_2$, *diagonal matrices* $Z_0=diag\{Z_{01},Z_{02},\cdots,Z_{0\mathscr{N}}\}$, $Z_1=diag\{Z_{11},Z_{12},\cdots,Z_{1\mathscr{N}}\}$ *exist that make the following LMIs true for any* $d_f\in(0,d]$,

$$\Delta_1(d_f)=\begin{bmatrix} \Phi_1+d_f\Phi_2 & \sqrt{d_f}\Pi_{10}^{T}N_1 & \sqrt{d_f}\Pi_{10}^{T}N_2 \\ * & -\mathscr{R}_2 & 0 \\ * & * & -3\mathscr{R}_2 \end{bmatrix}<0, \tag{11}$$

$$\Delta_2(d_f)=\begin{bmatrix} \Phi_1+d_f\Phi_3 & \sqrt{d_f}\Pi_{9}^{T}M_1 & \sqrt{d_f}\Pi_{9}^{T}M_2 \\ * & -\mathscr{R}_1 & 0 \\ * & * & -3\mathscr{R}_1 \end{bmatrix}<0, \tag{12}$$

where

$$\begin{aligned} \Phi_1=&Sym\Big\{-\rho\Pi_{11}^{T}\Lambda_1\Pi_{11}+\Pi_1^{T}(\mathscr{Q}_1\Pi_2+\mathscr{Q}_2\Pi_3)+\Lambda_2+\Pi_9^{T}M_1\Pi_{14}+\Pi_9^{T}M_2\Pi_{15} \\ &+\Pi_{10}^{T}N_1\Pi_{16}+\Pi_{10}^{T}N_2\Pi_{17}-e_1^{T}Z_0e_8+e_1^{T}Z_0e_6+e_1^{T}Z_0\Pi_{12}+e_1^{T}Z_1e_2 \\ &-\gamma e_8^{T}Z_0e_8+\gamma e_8^{T}Z_0e_6+\gamma e_8^{T}Z_0\Pi_{12}+\gamma e_8^{T}Z_1e_2\Big\}, \\ \Phi_2=&Sym\{\Pi_5^{T}(\mathscr{Q}_1\Pi_2+\mathscr{Q}_2\Pi_3)+\Pi_7^{T}\mathscr{Q}_1\Pi_4\}+e_8^{T}\mathscr{R}_1e_8, \\ \Phi_3=&Sym\{\Pi_6^{T}(\mathscr{Q}_1\Pi_2+\mathscr{Q}_2\Pi_3)+\Pi_8^{T}\mathscr{Q}_1\Pi_4\}+e_8^{T}\mathscr{R}_2e_8, \\ \Pi_1=&\begin{bmatrix} e_2^{T}-e_1^{T} & e_1^{T}-e_3^{T} \end{bmatrix}^{T}, \\ \Pi_2=&\begin{bmatrix} e_1^{T}-e_2^{T} & e_1^{T}-e_3^{T} \end{bmatrix}^{T}, \\ \Pi_3=&\begin{bmatrix} e_2^{T} & e_3^{T} \end{bmatrix}^{T}, \Pi_4=\begin{bmatrix} e_8^{T} & e_8^{T} \end{bmatrix}^{T}, \\ \Pi_5=&\begin{bmatrix} e_8^{T} & 0 \end{bmatrix}^{T}, \Pi_6=\begin{bmatrix} 0 & e_8^{T} \end{bmatrix}^{T}, \\ \Pi_7=&\begin{bmatrix} e_1^{T}-e_2^{T} & 0 \end{bmatrix}^{T}, \Pi_8=\begin{bmatrix} 0 & e_1^{T}-e_3^{T} \end{bmatrix}^{T}, \\ \Pi_9=&\begin{bmatrix} e_1^{T} & e_3^{T} & e_4^{T} \end{bmatrix}^{T}, \Pi_{10}=\begin{bmatrix} e_1^{T} & e_3^{T} & e_5^{T} \end{bmatrix}^{T}, \\ \Pi_{11}=&\begin{bmatrix} e_1^{T} & e_6^{T} \end{bmatrix}^{T}, \Pi_{12}=c(\mathscr{G}\otimes\mathscr{A})e_7, \\ \Pi_{13}=&e_1-e_7, \Pi_{14}=(\flat_1-\flat_2)\Pi_9, \\ \Pi_{15}=&(2\flat_3-\flat_1-\flat_2)\Pi_9, \Pi_{16}=(\flat_1-\flat_2)\Pi_{10}, \\ \Pi_{17}=&(2\flat_3-\flat_1-\flat_2)\Pi_{10}, \\ \Lambda_1=&\begin{bmatrix} \frac{\amalg\otimes(S_1^{T}S_2+S_2^{T}S_1)}{2} & \frac{-\amalg\otimes(S_1^{T}+S_2^{T})}{2} \\ * & \amalg \end{bmatrix}, \\ \Lambda_2=&\ell^2e_8^{T}\mathscr{W}_1e_8-\Pi_{13}^{T}\mathscr{W}_1\Pi_{13}+e_1^{T}\mathscr{W}_2e_1-e_7^{T}\mathscr{W}_2e_7+e_1^{T}\mathscr{P}e_8, \end{aligned}$$

then, for any initial condition $\hat{e}(\hat{t}_0)$, *FSs* (1) *and LS* (3) *could realize asymptotical synchronization, i.e., ES* (6) *is stable, and the formula* $\daleth=Z_0^{-1}Z_1$ *yields the controlling gain matrix.*

Proof Choose Lyapunov-Krasovskii functions for ES (6) as follows:

$$\mathscr{K}(\hat{t})=\sum_{p=1}^{4}\mathscr{K}_p(\hat{t}),\ \hat{t}\in[\hat{t}_f,\hat{t}_{f+1}), \tag{13}$$

in which

$$\begin{aligned} \mathscr{K}_1(\hat{t})=&2\ell\int_{-\ell}^{0}\int_{\hat{t}+\varkappa}^{\hat{t}}\dot{\hat{e}}^{T}(\wp)\mathscr{W}_1\dot{\hat{e}}(\wp)d\wp d\varkappa \\ &+2\int_{\hat{t}-\ell}^{\hat{t}}\hat{e}^{T}(\wp)\mathscr{W}_2\hat{e}(\wp)d\wp+\hat{e}^{T}(\hat{t})\mathscr{P}\hat{e}(\hat{t}), \\ \mathscr{K}_2(\hat{t})=&2\xi_3^{T}(\hat{t})\big[\mathscr{Q}_1\xi_2(\hat{t})+\mathscr{Q}_2\xi_1(\hat{t})\big], \\ \mathscr{K}_3(\hat{t})=&(\hat{t}_{f+1}-\hat{t})\int_{\hat{t}_f}^{\hat{t}}\dot{\hat{e}}^{T}(\wp)\mathscr{R}_1\dot{\hat{e}}(\wp)d\wp, \\ \mathscr{K}_4(\hat{t})=&-(\hat{t}-\hat{t}_f)\int_{\hat{t}}^{\hat{t}_{f+1}}\dot{\hat{e}}^{T}(\wp)\mathscr{R}_2\dot{\hat{e}}(\wp)d\wp. \end{aligned}$$

Taking into account the trajectory of ES (6), the differentiation of $\mathscr{K}(\hat{t})$ results in

$$\begin{aligned}
\dot{\mathscr{K}}_1(\hat{t}) &= 2\ell^2\dot{\hat{e}}^T(\hat{t})\mathscr{W}_1\dot{\hat{e}}(\hat{t}) - 2[\hat{e}(\hat{t}) \\
&- \hat{e}(\hat{t}-\ell)]^T\mathscr{W}_1[\hat{e}(\hat{t}) - \hat{e}(\hat{t}-\ell)] + 2\hat{e}^T(\hat{t})\mathscr{W}_2\hat{e}(\hat{t}) \\
&- 2\hat{e}^T(\hat{t}-\ell)\mathscr{W}_2\hat{e}(\hat{t}-\ell) + 2\hat{e}^T(\hat{t})\mathscr{P}\dot{\hat{e}}(\hat{t}) \\
&= 2\xi^T(\hat{t})\{\ell^2 e_8^T\mathscr{W}_1 e_8 - \Pi_{13}^T\mathscr{W}_1\Pi_{13} + e_1^T\mathscr{W}_2 e_1 - e_7^T\mathscr{W}_2 e_7 + e_1^T\mathscr{P}e_8\}\xi(\hat{t}), \\
\dot{\mathscr{K}}_2(\hat{t}) &= 2\xi^T(\hat{t})\{\Pi_1^T(\mathscr{Q}_1\Pi_2 + \mathscr{Q}_2\Pi_3) + (\hat{t}_{f+1} - \hat{t}) \\
&\times [\Pi_5^T(\mathscr{Q}_1\Pi_2 + \mathscr{Q}_2\Pi_3) + \Pi_7\mathscr{Q}_1\Pi_4] \\
&+ (\hat{t} - \hat{t}_f) \times [\Pi_6^T(\mathscr{Q}_1\Pi_2 + \mathscr{Q}_2\Pi_3) + \Pi_8^T\mathscr{Q}_1\Pi_4]\}\xi(\hat{t}), \\
\dot{\mathscr{K}}_3(\hat{t}) &= (\hat{t}_{f+1} - \hat{t})\dot{\hat{e}}^T(\hat{t})\mathscr{R}_1\dot{\hat{e}}(\hat{t}) + \mathscr{J}_1, \\
\dot{\mathscr{K}}_4(\hat{t}) &= (\hat{t} - \hat{t}_f)\dot{\hat{e}}^T(\hat{t})\mathscr{R}_2\dot{\hat{e}}(\hat{t}) + \mathscr{J}_2,
\end{aligned}$$

with $\mathscr{J}_1 = -\int_{\hat{t}_f}^{\hat{t}} \dot{\hat{e}}^T(\wp)\mathscr{R}_1\dot{\hat{e}}(\wp)d\wp$ and $\mathscr{J}_2 = -\int_{\hat{t}}^{\hat{t}_{f+1}} \dot{\hat{e}}^T(\wp)\mathscr{R}_2\dot{\hat{e}}(\wp)d\wp$.

Apply Lemma 3 to $\mathscr{J}_1$ and $\mathscr{J}_2$, then

$$\begin{aligned}
\dot{\mathscr{K}}_3(\hat{t}) &\le (\hat{t}_{f+1} - \hat{t})\xi^T(\hat{t})e_8^T\mathscr{R}_1 e_8\xi(\hat{t}) \\
&+ \xi^T(\hat{t})\Pi_9^T\left[(\hat{t} - \hat{t}_f)\left(M_1\mathscr{R}_1^{-1}M_1^T + \frac{1}{3}M_2\mathscr{R}_1^{-1}M_2^T\right)\right. \\
&\left. + Sym\{M_1(\flat_1 - \flat_2) + M_2(2\flat_3 - \flat_1 - \flat_2)\}\right]\Pi_9\xi(\hat{t}), \\
\dot{\mathscr{K}}_4(\hat{t}) &\le (\hat{t} - \hat{t}_f)\xi^T(\hat{t})e_8^T\mathscr{R}_2 e_8\xi(\hat{t}) \\
&+ \xi^T(\hat{t})\Pi_{10}^T\left[(\hat{t}_{f+1} - \hat{t})\left(N_1\mathscr{R}_2^{-1}N_1^T + \frac{1}{3}N_2\mathscr{R}_2^{-1}N_2^T\right)\right. \\
&\left. + Sym\{N_1(\flat_1 - \flat_2) + N_2(2\flat_3 - \flat_1 - \flat_2)\}\right]\Pi_{10}\xi(\hat{t}),
\end{aligned}$$

for any matrices with the proper dimensions, $M_i, N_i, i = 1, 2$, are acceptable.

As an additional feature, the statement that follows is true for a scalar $\rho > 0$ according to Assumption 1:

$$0 \le -2\rho\begin{bmatrix}\hat{e}(\hat{t}) \\ \beth(\hat{e}(\hat{t}))\end{bmatrix}^T\begin{bmatrix}\frac{\beth\otimes(S_1^TS_2 + S_2^TS_1)}{2} & \frac{-\beth\otimes(S_1^T + S_2^T)}{2} \\ * & \beth\end{bmatrix}^T\begin{bmatrix}\hat{e}(\hat{t}) \\ \beth(\hat{e}(\hat{t}))\end{bmatrix},$$

ie.,

$$0 \le -2\rho\xi^T(\hat{t})\Pi_{11}^T\begin{bmatrix}\frac{\beth\otimes(S_1^TS_2 + S_2^TS_1)}{2} & \frac{-\beth\otimes(S_1^T + S_2^T)}{2} \\ * & \beth\end{bmatrix}^T\Pi_{11}\xi(\hat{t}). \tag{14}$$

According to ES (6), for any diagonal matrix Z_0, positive scalar γ,

$$\begin{aligned}
0 = 2\left[\hat{e}^T(\hat{t})Z_0 + \gamma\dot{\hat{e}}^T(\hat{t})Z_0\right]&\left[-\dot{\hat{e}}(\hat{t}) + \beth(\hat{e}(\hat{t}))\right. \\
&\left. + c(\mathscr{G}\otimes\mathscr{A})\hat{e}(\hat{t}-\ell) + \gimel\hat{e}(\hat{t}_f)\right].
\end{aligned} \tag{15}$$

Define $Z_0\gimel = Z_1$, add the right end of (14) and (15) to $\dot{\mathscr{K}}(\hat{t})$ and attain

$$\dot{\mathscr{K}}(\hat{t}) \le \xi^T(\hat{t})\left[\frac{\hat{t} - \hat{t}_f}{d_f}\hat{\Delta}_2(d_f) + \frac{\hat{t}_{f+1} - \hat{t}}{d_f}\hat{\Delta}_1(d_f)\right]\xi(\hat{t}),$$

where

$$\begin{aligned}
\hat{\Delta}_1(d_f) &= \Phi_1 + d_f\Phi_2 + d_f\Pi_{10}^T\left(N_1\mathscr{R}_2^{-1}N_1^T + \frac{1}{3}N_2\mathscr{R}_2^{-1}N_2^T\right)\Pi_{10}, \\
\hat{\Delta}_2(d_f) &= \Phi_1 + d_f\Phi_3 + d_f\Pi_9^T\left(M_1\mathscr{R}_1^{-1}M_1^T + \frac{1}{3}M_2\mathscr{R}_1^{-1}M_2^T\right)\Pi_9.
\end{aligned}$$

Depending on Schur complement, assume that $\hat{\Delta}_1(d_f) < 0$ and $\hat{\Delta}_2(d_f) < 0$, which are equal to (11) and (12), correspondingly. After that $\dot{\mathscr{K}}(\hat{t}) \le 0$ follows, and ES (6) is therefore stable according to Seuret's theorem 1 [24]. □

Remark 4 Here, the continuous function (13) containing information from both sides of the sampling interval is proposed by combining the two-sided looped-function theory in [24], as well as the time-dependent continuous Lyapunov functional theory in [36], where state information $\hat{e}(\hat{t}_f)$, $\hat{e}(\hat{t})$, and $\hat{e}(\hat{t}_{f+1})$ are fully utilized, in addition to the integrating states $\int_{\hat{t}}^{\hat{t}_f}\hat{e}(\wp)d\wp$ and $\int_{\hat{t}}^{\hat{t}_{f+1}}\hat{e}(\wp)d\wp$. Taking advantage of information from these states is extremely beneficial to producing less conservative results. Yet another contrast to earlier studies on the synchronization of CDNs with sampling data, for instance, those in [2–4, 7, 16], the presence of $\mathscr{K}_2(\hat{t})$, where the matrices $\mathscr{Q}_1$ and $\mathscr{Q}_2$ are not positively definite, makes the constraint on the function (13) weaker and zero at the sampling time. Therefore, the Lyapunov functions $\mathscr{K}_1(\hat{t})$, $\mathscr{K}_3(\hat{t})$ and $\mathscr{K}_4(\hat{t})$ proposed in (13) are novel.

FSs (1) is thus transformed into the following model if the parameter ℓ is equal to 0,

$$\begin{cases}
\dot{e}_p(\hat{t}) = \pounds(e_p(\hat{t})) + c\sum_{q=1,q\ne p}^{\mathscr{N}}\mathscr{G}_{pq}\mathscr{A}(e_q(\hat{t}) - e_p(\hat{t})) + u_p(\hat{t}), \\
y_p(\hat{t}) = \eth e_p(\hat{t}), p = 1, 2, \ldots, \mathscr{N}.
\end{cases} \tag{16}$$

Theorem 1's parameter ℓ can be set to 0 to provide the following inference:

Corollary 1 *For given positive constants d, ρ, γ, when positive definite and symmetric matrices $\mathscr{W}_1 > 0, \mathscr{W}_2 > 0, \mathscr{P} > 0, \mathscr{R}_1 > 0, \mathscr{R}_2 > 0$, matrices $\mathscr{Q}_1, \mathscr{Q}_2, M_1, M_2, N_1, N_2$, diagonal matrices $Z_0 = diag\{Z_{01}, Z_{02}, \cdots, Z_{0\mathscr{N}}\}$, $Z_1 = diag\{Z_{11}, Z_{12}, \cdots, Z_{1\mathscr{N}}\}$ exist that make the following LMIs true for any $d_f \in (0, d]$,*

$$\Delta_1(d_f)=\begin{bmatrix}\Phi_1+d_f\Phi_2 & \sqrt{d_f}\Pi_{10}^T N_1 & \sqrt{d_f}\Pi_{10}^T N_2\\ * & -\mathscr{R}_2 & 0\\ * & * & -3\mathscr{R}_2\end{bmatrix}<0, \quad (17)$$

$$\Delta_2(d_f)=\begin{bmatrix}\Phi_1+d_f\Phi_3 & \sqrt{d_f}\Pi_9^T M_1 & \sqrt{d_f}\Pi_9^T M_2\\ * & -\mathscr{R}_1 & 0\\ * & * & -3\mathscr{R}_1\end{bmatrix}<0, \quad (18)$$

where

$$\begin{aligned}\Phi_1 =& Sym\Big\{-\rho\Pi_{11}^T\Lambda_1\Pi_{11}+\Pi_1^T(\mathscr{Q}_1\Pi_2+\mathscr{Q}_2\Pi_3)+\Lambda_2+\Pi_9^T M_1\Pi_{14}+\Pi_9^T M_2\Pi_{15}\\ &+\Pi_{10}^T N_1\Pi_{16}+\Pi_{10}^T N_2\Pi_{17}-e_1^T Z_0 e_8+e_1^T Z_0 e_6+e_1^T Z_0\Pi_{12}+e_1^T Z_1 e_2\\ &-\gamma e_8^T Z_0 e_8+\gamma e_8^T Z_0 e_6+\gamma e_8^T Z_0\Pi_{12}+\gamma e_8^T Z_1 e_2\Big\},\\ \Phi_2 =& Sym\{\Pi_5^T(\mathscr{Q}_1\Pi_2+\mathscr{Q}_2\Pi_3)+\Pi_7^T\mathscr{Q}_1\Pi_4\}+e_8^T\mathscr{R}_1 e_8,\\ \Phi_3 =& Sym\{\Pi_6^T(\mathscr{Q}_1\Pi_2+\mathscr{Q}_2\Pi_3)+\Pi_8^T\mathscr{Q}_1\Pi_4\}+e_8^T\mathscr{R}_2 e_8,\\ \Lambda_2 =& -\Pi_{13}^T\mathscr{W}_1\Pi_{13}+e_1^T\mathscr{W}_2 e_1-e_7^T\mathscr{W}_2 e_7+e_1^T\mathscr{P}e_8,\end{aligned}$$

where $\Lambda_1, \Pi_i, i=1,2,\ldots,17$, *are defined by Theorem* 1, *then, given any starting situation* $\hat{e}(\hat{t}_0)$, *FSs* (16) *and LS* (3) *could realize asymptotical synchronization, and the formula* $\mathfrak{I}=Z_0^{-1}Z_1$ *yields the controlling gain matrix.*

4 Sampled-data exponential synchronization analysis

In this part, the exponential stability of ES (6) under the data sampling controller in the form of (4) is studied by creating a Lyapunov function depending on sampling times. The following necessary designations on behalf of vectors and matrices are presented for simplicity:

$$\eta(\hat{t})=col\left\{\hat{e}(\hat{t}),\hat{e}(\hat{t}_f),\mathfrak{I}(\hat{e}(\hat{t})),\hat{e}(\hat{t}-\ell),\dot{\hat{e}}(\hat{t}),\int_{\hat{t}_f}^{\hat{t}}\hat{e}(\wp)d\wp\right\},$$

$$e_q=\left[0_{n\times(q-1)n}\ \amalg_n\ 0_{n\times(6-q)n}\right], q=1,2,\ldots,6.$$

Theorem 2 *With respect to the supplied positive scalars* a,d,ℓ,ρ,γ, *if symmetric and positive definite matrices* $\mathscr{P}>0, \mathscr{Q}_1>0, \mathscr{Z}_1>0, \begin{bmatrix}\mathscr{Z}_1 & \mathscr{Z}_2\\ * & \mathscr{Z}_3\end{bmatrix}>0, \mathfrak{O}_1>0$, matrices $\mathscr{Y}, \mathscr{Y}_1, M_1, M_2$, *diagonal matrices* $R_0=diag\{R_{01},R_{02},\cdots,R_{0\mathscr{N}}\}$, $R_1=diag\{R_{11},R_{12},\cdots,R_{1\mathscr{N}}\}$ *exist that make the following LMIs true for any* $d_f\in(0,d]$,

$$-\begin{bmatrix}\mathscr{P}+d\dfrac{\mathscr{Y}+\mathscr{Y}^T}{2}+e^{-2ad}\mathfrak{O}_1 & \Phi_1-e^{-2ad}\mathfrak{O}_1\\ * & \Phi_2+e^{-2ad}\mathfrak{O}_1\end{bmatrix}<0, \quad (19)$$

$$\Delta_1(d_f)=\begin{bmatrix}\Xi_1+d_f\Xi_2 & \sqrt{2}e^{-a\ell}e_1^T\mathscr{Z}_2-\sqrt{2}e^{-a\ell}e_4^T\mathscr{Z}_2\\ * & -\mathscr{Z}_3\end{bmatrix}<0, \quad (20)$$

$$\Delta_2(d_f)=\begin{bmatrix}\Xi_1 & \sqrt{d_f}e^{-ad}\Pi_2^T M_1 & \sqrt{d_f}e^{-ad}\Pi_2^T M_2 & \sqrt{2}e^{-a\ell}e_1^T\mathscr{Z}_2-\sqrt{2}e^{-a\ell}e_4^T\mathscr{Z}_2\\ * & -\mathfrak{O}_1 & 0 & 0\\ * & * & -3\mathfrak{O}_1 & 0\\ * & * & * & -\mathscr{Z}_3\end{bmatrix}<0, \quad (21)$$

where

$$\begin{aligned}\Xi_1 =& Sym\Big\{e_1^T\mathscr{P}e_5+ae_1^T\mathscr{P}e_1+e_1^T\mathscr{Q}_1e_1-e^{-2a\ell}e_4^T\mathscr{Q}_1e_4+\ell^2e_5^T\mathscr{Z}_1e_5-\frac{1}{2}\Phi_5\\ &+e^{-2ad}\Pi_2^T M_1\Pi_3+e^{-2ad}\Pi_2^T M_2\Pi_4+\Phi_4-\rho\Pi_5^T\Phi_3\Pi_5-e_1^T R_0e_5+e_1^T R_0e_3\\ &+e_1^T R_0\Pi_1+e_1^T R_1e_2-\gamma e_5^T R_0e_5+\gamma e_5^T R_0e_3+\gamma e_5^T R_0\Pi_1+\gamma e_5^T R_1e_2\Big\},\\ \Xi_2 =& Sym\Big\{e_5^T\mathfrak{O}_1e_5+a\Phi_5+\frac{1}{2}e_1^T\mathscr{Y}e_5+\frac{1}{2}e_5^T\mathscr{Y}e_1-e_5^T\mathscr{Y}e_2+e_5^T\mathscr{Y}_1e_2\Big\},\\ \Pi_1 =& c(\mathscr{G}\otimes\mathscr{A})e_4,\Pi_2=[e_1^T\ e_2^T\ e_6^T]^T,\\ \Pi_3 =& (\flat_1-\flat_2)\Pi_2,\Pi_4=(2\flat_3-\flat_1-\flat_2)\Pi_2,\Pi_5=[e_1^T\ e_3^T]^T,\\ \Phi_1 =& -d\mathscr{Y}+d\mathscr{Y}_1,\\ \Phi_2 =& -d\mathscr{Y}_1-d\mathscr{Y}_1^T+d\frac{\mathscr{Y}+\mathscr{Y}^T}{2},\\ \Phi_3 =& \begin{bmatrix}\dfrac{\amalg\otimes(S_1^TS_2+S_2^TS_1)}{2} & \dfrac{-\amalg\otimes(S_1^T+S_2^T)}{2}\\ * & \amalg\end{bmatrix},\\ \Phi_4 =& -e^{-2a\ell}e_1^T\mathscr{Z}_1e_1+\ell^2e^{-2a\ell}e_1^T\mathscr{Z}_3e_1+2\ell e^{-2a\ell}e_1^T\mathscr{Z}_2e_1+2e^{-2a\ell}e_1^T\mathscr{Z}_1e_4\\ &-2\ell e^{-2a\ell}e_4^T\mathscr{Z}_2e_1-e^{-2a\ell}e_4^T\mathscr{Z}_1e_4,\\ \Phi_5 =& e_1^T\mathscr{Y}e_1-2e_1^T\mathscr{Y}e_2+2e_1^T\mathscr{Y}_1e_2-2e_2^T\mathscr{Y}_1e_2+e_2^T\mathscr{Y}e_2,\end{aligned}$$

then, FSs (1) *and LS* (3) *could realize exponential synchronization, i.e., ES* (6) *is exponentially stable, and the formula* $\mathfrak{I}=R_0^{-1}R_1$ *yields the controlling gain matrix.*

Proof Consider LKFs for ES (6) below:

$$\mathscr{K}(\hat{t})=\sum_{p=1}^{5}\mathscr{K}_p(\hat{t}),\hat{t}\in[\hat{t}_f,\hat{t}_{f+1}), \quad (22)$$

in which

$$\mathscr{K}_1(\hat{t}) = e^{2a\hat{t}}\hat{e}^T(\hat{t})\mathscr{P}\hat{e}(\hat{t}),$$

$$\mathscr{K}_2(\hat{t}) = 2\int_{\hat{t}-\ell}^{\hat{t}} e^{2a\wp}\hat{e}^T(\wp)\mathscr{Q}_1\hat{e}(\wp)d\wp,$$

$$\mathscr{K}_3(\hat{t}) = 2\ell\int_{-\ell}^{0}\int_{\hat{t}+\varkappa}^{\hat{t}} e^{2a\wp}\dot{\hat{e}}^T(\wp)\mathscr{Z}_1\dot{\hat{e}}(\wp)d\wp d\varkappa,$$

$$\mathscr{K}_4(\hat{t}) = (\hat{t}_{f+1}-\hat{t})\int_{\hat{t}_f}^{\hat{t}} e^{2a\wp}\dot{\hat{e}}^T(\wp)\mathfrak{V}_1\dot{\hat{e}}(\wp)d\wp,$$

$$\mathscr{K}_5(\hat{t}) = (\hat{t}_{f+1}-\hat{t})e^{2a\hat{t}}\eta_2^T\mathcal{W}\eta_2,\ \mathcal{W} = \begin{bmatrix} \frac{\mathscr{Y}+\mathscr{Y}^T}{2} & -\mathscr{Y}+\mathscr{Y}_1 \\ * & -\mathscr{Y}_1-\mathscr{Y}_1^T+\frac{\mathscr{Y}+\mathscr{Y}^T}{2}\end{bmatrix},$$

$$\eta_2 = \begin{bmatrix}\hat{e}(\hat{t})\\ \hat{e}(\hat{t}_f)\end{bmatrix}.$$

Already, the matrices $\mathscr{Q}_1$ and $\mathscr{Z}_1$ are required to remain positively defined. Afterwards,

$$\begin{aligned}\mathscr{K}(\hat{t}) &\geq \mathscr{K}_1(\hat{t})+\mathscr{K}_4(\hat{t})+\mathscr{K}_5(\hat{t})\\ &\geq e^{2a\hat{t}}\hat{e}(\hat{t})^T\mathscr{P}\hat{e}(\hat{t}) + e^{2a\hat{t}}(\hat{t}_{f+1}-\hat{t})\begin{bmatrix}\hat{e}(\hat{t})\\ \hat{e}(\hat{t}_f)\end{bmatrix}^T\left(\frac{1}{d}\mathcal{T}+\mathcal{W}\right)\begin{bmatrix}\hat{e}(\hat{t})\\ \hat{e}(\hat{t}_f)\end{bmatrix}\\ &= e^{2a\hat{t}}\begin{bmatrix}\hat{e}(\hat{t})\\ \hat{e}(\hat{t}_f)\end{bmatrix}^T\hat{\Omega}\begin{bmatrix}\hat{e}(\hat{t})\\ \hat{e}(\hat{t}_f)\end{bmatrix},\end{aligned} \tag{23}$$

in which Jensen inequality is utilized with notations

$$\mathcal{T} = e^{-2ad}\begin{bmatrix}\mathfrak{V}_1 & -\mathfrak{V}_1\\ * & \mathfrak{V}_1\end{bmatrix},$$
$$\hat{\Omega} = \frac{\hat{t}_{f+1}-\hat{t}}{d_f}(\hat{\Upsilon}+\frac{d_f}{d}\mathcal{T}+d_f\mathcal{W})+\frac{\hat{t}-\hat{t}_f}{d_f}\hat{\Gamma},\quad \hat{\Upsilon} = \begin{bmatrix}\mathscr{P} & 0\\ * & 0\end{bmatrix}. \tag{24}$$

Let's perform the modification shown below:

$$\hat{\Upsilon}+\frac{d_f}{d}\mathcal{T}+d_f\mathcal{W} = \frac{d_f}{d}(\hat{\Upsilon}+\mathcal{T}+d\mathcal{W})+\frac{d-d_f}{d}\hat{\Upsilon}.$$

By Schur complement, Eq. (19) implies

$$\hat{\Upsilon}+\mathcal{T}+d\mathcal{W} > 0.$$

Assuming that $\mathscr{P} > 0$ and (19), then there is a tiny enough scalar $\beta > 0$ to allow for $\hat{\Upsilon} > \beta diag\{\amalg, 0\}$ and $\hat{\Upsilon}+\mathcal{T}+d\mathcal{W} > \beta diag\{\amalg, \amalg\}$. In accordance with Eqs (23) and (24),

$$\mathscr{K}(\hat{t}) \geq \beta e^{2a\hat{t}}||\hat{e}(\hat{t})||^2. \tag{25}$$

□

It should be noted that the methods described in [10, 16], and [17] served as inspiration for Lyapunov functional (22), especially the important terms $\mathscr{K}_4(\hat{t})$ and $\mathscr{K}_5(\hat{t})$. The findings indicate that $\mathscr{K}_4(\hat{t})$ and $\mathscr{K}_5(\hat{t})$ disappear at $\hat{t} = \hat{t}_f$ or $\hat{t}_{f+1}$. $\mathscr{K}(\hat{t})$ is therefore continuous for the reason that $\lim_{\hat{t}\to\hat{t}_f}\mathscr{K}(\hat{t}) = \mathscr{K}(\hat{t}_f)$. As a result, it is appropriate to choose the Lyapunov function $\mathscr{K}(\hat{t})$ described in (22) for ES (6). For $\hat{t}\in[\hat{t}_f, \hat{t}_{f+1})$, calculate and obtain the value of the time derivative for $\mathscr{K}(\hat{t})$ across the track on ES (6) below:

$$\dot{\mathscr{K}}_1(\hat{t}) = 2e^{2a\hat{t}}\eta^T(\hat{t})(e_1^T\mathscr{P}e_5+ae_1^T\mathscr{P}e_1)\eta(\hat{t}),$$

$$\dot{\mathscr{K}}_2(\hat{t}) = 2e^{2a\hat{t}}\eta^T(\hat{t})(e_1^T\mathscr{Q}_1e_1-e^{-2a\ell}e_4^T\mathscr{Q}_1e_4)\eta(\hat{t}),$$

$$\begin{aligned}\dot{\mathscr{K}}_3(\hat{t}) &= -2\ell\int_{\hat{t}-\ell}^{\hat{t}} e^{2a\wp}\dot{\hat{e}}^T(\wp)\mathscr{Z}_1\dot{\hat{e}}(\wp)d\wp + 2\ell^2e^{2a\hat{t}}\dot{\hat{e}}^T(\hat{t})\mathscr{Z}_1\dot{\hat{e}}(\hat{t})\\ &\leq -2e^{2a\hat{t}}e^{-2a\ell}\ell\int_{\hat{t}-\ell}^{\hat{t}}\dot{\hat{e}}^T(\wp)\mathscr{Z}_1\dot{\hat{e}}(\wp)d\wp + 2e^{2a\hat{t}}\eta^T(\hat{t})\ell^2e_5^T\mathscr{Z}_1e_5\eta(\hat{t}),\end{aligned}$$

$$\begin{aligned}\dot{\mathscr{K}}_4(\hat{t}) &= -\int_{\hat{t}_f}^{\hat{t}} e^{2a\wp}\dot{\hat{e}}^T(\wp)\mathfrak{V}_1\dot{\hat{e}}(\wp)d\wp + (\hat{t}_{f+1}-\hat{t})e^{2a\hat{t}}\dot{\hat{e}}^T(\hat{t})\mathfrak{V}_1\dot{\hat{e}}(\hat{t})\\ &\leq -e^{2a\hat{t}}e^{-2ad}\int_{\hat{t}_f}^{\hat{t}}\dot{\hat{e}}^T(\wp)\mathfrak{V}_1\dot{\hat{e}}(\wp)d\wp + (\hat{t}_{f+1}-\hat{t})e^{2a\hat{t}}\eta^T(\hat{t})e_5^T\mathfrak{V}_1e_5\eta(\hat{t}),\end{aligned}$$

$$\begin{aligned}\dot{\mathscr{K}}_5(\hat{t}) = &-e^{2a\hat{t}}\eta^T(\hat{t})\begin{bmatrix}e_1\\ e_2\end{bmatrix}^T\mathcal{W}\begin{bmatrix}e_1\\ e_2\end{bmatrix}\eta(\hat{t})\\ &+e^{2a\hat{t}}(\hat{t}_{f+1}-\hat{t})\eta^T(\hat{t})2a\begin{bmatrix}e_1\\ e_2\end{bmatrix}^T\mathcal{W}\begin{bmatrix}e_1\\ e_2\end{bmatrix}\eta(\hat{t})\\ &+e^{2a\hat{t}}(\hat{t}_{f+1}-\hat{t})\eta^T(\hat{t})e_1^T(\mathscr{Y}+\mathscr{Y}^T)e_5\eta(\hat{t})\\ &+e^{2a\hat{t}}(\hat{t}_{f+1}-\hat{t})\eta^T(\hat{t})2e_5^T(-\mathscr{Y}+\mathscr{Y}_1)e_2\eta(\hat{t}).\end{aligned}$$

According to Lemmas 3 and 5,

$$\begin{aligned}-\int_{\hat{t}_f}^{\hat{t}}\dot{\hat{e}}^T(\wp)\mathfrak{V}_1\dot{\hat{e}}(\wp)d\wp &\leq \eta^T(\hat{t})\Pi_2^T\Big[(\hat{t}-\hat{t}_f)\Big(M_1\mathfrak{V}_1^{-1}M_1^T+\frac{1}{3}M_2\mathfrak{V}_1^{-1}M_2^T\Big)\\ &+Sym\{M_1(\flat_1-\flat_2)+M_2(2\flat_3-\flat_1-\flat_2)\}\Big]\Pi_2\eta(\hat{t}),\\ -2e^{2a\hat{t}}e^{-2a\ell}\ell\int_{\hat{t}-\ell}^{\hat{t}}\dot{\hat{e}}^T(\wp)\mathscr{Z}_1\dot{\hat{e}}(\wp)d\wp &\leq 2e^{2a\hat{t}}e^{-2a\ell}\eta^T(\hat{t})\begin{bmatrix}e_1\\ e_4\end{bmatrix}^T\Upsilon\begin{bmatrix}e_1\\ e_4\end{bmatrix}\eta(\hat{t}),\end{aligned}$$

where

$$\begin{aligned}\Upsilon_{11} &= \mathscr{Z}_2\mathscr{Z}_3^{-1}\mathscr{Z}_2^T-\mathscr{Z}_1+\ell^2\mathscr{Z}_3+2\ell\mathscr{Z}_2,\\ \Upsilon_{12} &= -\mathscr{Z}_2\mathscr{Z}_3^{-1}\mathscr{Z}_2^T+\mathscr{Z}_1-\ell\mathscr{Z}_2^T,\\ \Upsilon_{22} &= \mathscr{Z}_2\mathscr{Z}_3^{-1}\mathscr{Z}_2^T-\mathscr{Z}_1.\end{aligned}$$

Additionally, the statement that follows is true for a scalar $\rho > 0$ through Assumption 1:

$$0 \leq -2\rho e^{2a\hat{t}}\eta^T(\hat{t})\begin{bmatrix}e_1\\ e_3\end{bmatrix}^T\begin{bmatrix}\frac{\amalg\otimes(S_1^TS_2+S_2^TS_1)}{2} & \frac{-\amalg\otimes(S_1^T+S_2^T)}{2}\\ * & \amalg\end{bmatrix}\begin{bmatrix}e_1\\ e_3\end{bmatrix}\eta(\hat{t}). \tag{26}$$

According to ES (6),

$$0 = 2e^{2a\hat{t}}\left[\hat{e}^T(\hat{t})R_0 + \gamma\dot{\hat{e}}^T(\hat{t})R_0\right]\left[-\dot{\hat{e}}(\hat{t}) + \mathfrak{A}(\hat{e}(\hat{t})) + c(\mathscr{G}\otimes\mathscr{A})\hat{e}(\hat{t}-\ell) + \mathfrak{I}\hat{e}(\hat{t}_f)\right]. \quad (27)$$

Define $R_0\mathfrak{I} = R_1$, add the right-side places from (26) and (27) to $\dot{\mathscr{K}}(\hat{t})$, then for $\hat{t} \in [\hat{t}_f, \hat{t}_{f+1})$,

$$\dot{\mathscr{K}}(\hat{t}) \le e^{2a\hat{t}}\eta^T(\hat{t})\left[\frac{\hat{t}-\hat{t}_f}{d_f}\hat{\Delta}_2(d_f) + \frac{\hat{t}_{f+1}-\hat{t}}{d_f}\hat{\Delta}_1(d_f)\right]\eta(\hat{t}),$$

with $\hat{\Delta}_1(d_f)$ and $\hat{\Delta}_2(d_f)$ are given below:

$$\begin{aligned}
\hat{\Delta}_1(d_f) &= \Xi_1 + d_f\Xi_2 + 2e^{-2a\ell}e_1^T\mathscr{Z}_2\mathscr{Z}_3^{-1}\mathscr{Z}_2^Te_1 \\
&- 4e^{-2a\ell}e_1^T\mathscr{Z}_2\mathscr{Z}_3^{-1}\mathscr{Z}_2^Te_4 + 2e^{-2a\ell}e_4^T\mathscr{Z}_2\mathscr{Z}_3^{-1}\mathscr{Z}_2^Te_4, \\
\hat{\Delta}_2(d_f) &= \Xi_1 + d_fe^{-2ad}\Pi_2^TM_1\mathfrak{O}_1^{-1}M_1^T\Pi_2 \\
&+ \frac{1}{3}d_fe^{-2ad}\Pi_2^TM_2\mathfrak{O}_1^{-1}M_2^T\Pi_2 \\
&\quad + 2e^{-2a\ell}e_1^T\mathscr{Z}_2\mathscr{Z}_3^{-1}\mathscr{Z}_2^Te_1 \\
&- 4e^{-2a\ell}e_1^T\mathscr{Z}_2\mathscr{Z}_3^{-1}\mathscr{Z}_2^Te_4 \\
&+ 2e^{-2a\ell}e_4^T\mathscr{Z}_2\mathscr{Z}_3^{-1}\mathscr{Z}_2^Te_4.
\end{aligned}$$

Meanwhile, depending on Schur complement, it's concluded from (20) and (21) that $\hat{\Delta}_1(d_f) < 0$, $\hat{\Delta}_2(d_f) < 0$. Then,

$$\dot{\mathscr{K}}(\hat{t}) \le 0, \hat{t} \in [\hat{t}_f, \hat{t}_{f+1}).$$

Therefore,

$$\mathscr{K}(0) \ge \mathscr{K}(\hat{t}_1) \ge \cdots \ge \mathscr{K}(\hat{t}_{f-1}) \ge \mathscr{K}(\hat{t}_f) \ge \mathscr{K}(\hat{t}). \quad (28)$$

Notice $\mathscr{K}_4(0) = 0$ and $\mathscr{K}_5(0) = 0$, indicating that

$$\begin{aligned}
\mathscr{K}(0) &= \sum_{p=1}^{5}\mathscr{K}_p(0) \\
&\le \lambda_{max}(\mathscr{P})||\hat{e}(0)||^2 + 2\ell\lambda_{max}(\mathscr{Q}_1)\sup_{-\ell\le\Upsilon\le 0}\left\{||\hat{e}(\Upsilon)||^2\right\} \\
&\quad + 2\ell^3\lambda_{max}(\mathscr{Z}_1)\sup_{-\ell\le\Upsilon\le 0}\left\{||\dot{\hat{e}}(\Upsilon)||^2\right\} \\
&\le a_0\left(\sup_{-\ell\le\Upsilon\le 0}\left\{||\hat{e}(\Upsilon)||, ||\dot{\hat{e}}(\Upsilon)||\right\}\right)^2,
\end{aligned} \quad (29)$$

where

$$a_0 = \lambda_{max}(\mathscr{P}) + 2\ell\lambda_{max}(\mathscr{Q}_1) + 2\ell^3\lambda_{max}(\mathscr{Z}_1).$$

Focusing on (25), (28), and (29), we have

$$\beta e^{2a\hat{t}}||\hat{e}(\hat{t})||^2 \le a_0\left(\sup_{-\ell\le\Upsilon\le 0}\left\{||\hat{e}(\Upsilon)||, ||\dot{\hat{e}}(\Upsilon)||\right\}\right)^2,$$

which suggests

$$||\hat{e}(\hat{t})|| \le \sqrt{\frac{a_0}{\beta}}e^{-a\hat{t}}\sup_{-\ell\le\Upsilon\le 0}\left\{||\hat{e}(\Upsilon)||, ||\dot{\hat{e}}(\Upsilon)||\right\}. \quad (30)$$

From (30), it can be inferred that ES (6) has an exponentially stable decay rate of a.

Remark 5 Emphasize that we verify their positive characteristics by treating $\mathscr{K}_1$, $\mathscr{K}_2$, $\mathscr{K}_3$, $\mathscr{K}_4$, and $\mathscr{K}_5$ as a whole, in contrast to the current results in [3, 8, 16], which call for all the matrices with a symmetrical structure to be positively defined matrices. As a consequence, the matrices in the LKF's constraint are currently eased, which is a crucial factor toward lowering conservativeness. Additionally, based on the Lyapunov functional method depending on sampling times [10], the Lyapunov functioning (22) introduces the limitations $\mathscr{K}_4(\hat{t})$ and $\mathscr{K}_5(\hat{t})$ with respect to $\hat{t}_f$ and $\hat{t}_{f+1}$, which effectively lower the conservatism of the obtained results by making the most of the accessible sampling interval information.

Set the parameter a in Theorem 2 equal to 0, and we get the following inference:

Corollary 2 *With respect to the supplied positive scalars* d, ℓ, ρ, γ, *if symmetric and positive definite matrices* $\mathscr{P} > 0, \mathscr{Q}_1 > 0, \mathscr{Z}_1 > 0, \begin{bmatrix}\mathscr{Z}_1 & \mathscr{Z}_2 \\ * & \mathscr{Z}_3\end{bmatrix} > 0, \mathfrak{O}_1 > 0$, *matrices* $\mathscr{Y}, \mathscr{Y}_1, M_1, M_2$, *diagonal matrices* $R_0 = diag\{R_{01}, R_{02}, \cdots, R_{0\mathscr{N}}\}$, $R_1 = diag\{R_{11}, R_{12}, \cdots, R_{1\mathscr{N}}\}$ *exist that make the following LMIs true for any* $d_f \in (0, d]$,

$$-\begin{bmatrix}\mathscr{P} + d\dfrac{\mathscr{Y}+\mathscr{Y}^T}{2} + \mathfrak{O}_1 & \Phi_1 - \mathfrak{O}_1 \\ * & \Phi_2 + \mathfrak{O}_1\end{bmatrix} < 0, \quad (31)$$

$$\Delta_1(d_f) = \begin{bmatrix}\Xi_1 + d_f\Xi_2 & \sqrt{2}e_1^T\mathscr{Z}_2 - \sqrt{2}e_4^T\mathscr{Z}_2 \\ * & -\mathscr{Z}_3\end{bmatrix} < 0, \quad (32)$$

$$\Delta_2(d_f) = \begin{bmatrix}\Xi_1 & \sqrt{d_f}\Pi_2^TM_1 & \sqrt{d_f}\Pi_2^TM_2 & \sqrt{2}e_1^T\mathscr{Z}_2 - \sqrt{2}e_4^T\mathscr{Z}_2 \\ * & -\mathfrak{O}_1 & 0 & 0 \\ * & * & -3\mathfrak{O}_1 & 0 \\ * & * & * & -\mathscr{Z}_3\end{bmatrix} < 0, \quad (33)$$

where

$$\Xi_1 = Sym\Big\{ e_1^T \mathscr{P} e_5 + e_1^T \mathscr{Q}_1 e_1 - e_4^T \mathscr{Q}_1 e_4 + \ell^2 e_5^T \mathscr{Z}_1 e_5 - \frac{1}{2}\Phi_5 + \Pi_2^T M_1 \Pi_3 + \Pi_2^T M_2 \Pi_4 + \Phi_4 - \rho \Pi_5^T \Phi_3 \Pi_5 - e_1^T R_0 e_5 + e_1^T R_0 e_3 + e_1^T R_0 \Pi_1 + e_1^T R_1 e_2 - \gamma e_5^T R_0 e_5 + \gamma e_5^T R_0 e_3 + \gamma e_5^T R_0 \Pi_1 + \gamma e_5^T R_1 e_2 \Big\},$$

$$\Xi_2 = Sym\Big\{ e_5^T \mathfrak{V}_1 e_5 + \frac{1}{2} e_1^T \mathscr{Y} e_5 + \frac{1}{2} e_5^T \mathscr{Y} e_1 - e_5^T \mathscr{Y} e_2 + e_5^T \mathscr{Y}_1 e_2 \Big\},$$

$$\Pi_1 = c(\mathscr{G} \otimes \mathscr{A}) e_4, \Pi_2 = [e_1^T \ e_2^T \ e_6^T]^T,$$

$$\Pi_3 = (\flat_1 - \flat_2)\Pi_2, \Pi_4 = (2\flat_3 - \flat_1 - \flat_2)\Pi_2, \Pi_5 = [e_1^T \ e_3^T]^T,$$

$$\Phi_1 = -d\mathscr{Y} + d\mathscr{Y}_1,$$

$$\Phi_2 = -d\mathscr{Y}_1 - d\mathscr{Y}_1^T + d\frac{\mathscr{Y} + \mathscr{Y}^T}{2},$$

$$\Phi_3 = \begin{bmatrix} \frac{\amalg \otimes (S_1^T S_2 + S_2^T S_1)}{2} & \frac{-\amalg \otimes (S_1^T + S_2^T)}{2} \\ * & \amalg \end{bmatrix},$$

$$\Phi_4 = -e_1^T \mathscr{Z}_1 e_1 + \ell^2 e_1^T \mathscr{Z}_3 e_1 + 2\ell e_1^T \mathscr{Z}_2 e_1 + 2e_1^T \mathscr{Z}_1 e_4 - 2\ell e_4^T \mathscr{Z}_2 e_1 - e_4^T \mathscr{Z}_1 e_4,$$

$$\Phi_5 = e_1^T \mathscr{Y} e_1 - 2e_1^T \mathscr{Y} e_2 + 2e_1^T \mathscr{Y}_1 e_2 - 2e_2^T \mathscr{Y}_1 e_2 + e_2^T \mathscr{Y} e_2,$$

then, FSs (1) and LS (3) could realize exponential synchronization with a small enough decay rate, i.e., ES (6) is exponentially stable and has a sufficiently slow degradation rate, and the formula $\daleth = R_0^{-1} R_1$ *yields the controlling gain matrix.*

Remark 6 Due to the influence of digital feedback, sampling control is more suitable for practical applications than continuous control because it only uses the data of the state vector at a discrete time. Furthermore, compared with the memory sampling data controllers, the nonmemory sampled-data controllers are widely used in this article, which don't need the state value of the previous sampling time in the actual control process, thus improving the computation burden and load limitation. It should be pointed out that the problem of sampling synchronization control for delayed complex networks is solved, and the sufficient conditions for the existence of the sampled data controller are given, which are represented by LMIs and can be solved easily with standard numerical software. It should be noted that the LMIs given in Theorem 2 depend not only on the maximum sampling interval d but also on the decay rate α.

5 Numerical examples

Example 1 Think about FSs (1) with three follower systems. The matrix of inner connection as well as the matrix of outer connection, respectively, are provided as

$$\mathscr{A} = \begin{bmatrix} 1 & 0 \\ 0 & 1 \end{bmatrix}, \ \mathscr{G} = \begin{bmatrix} -1 & 0 & 1 \\ 0 & -1 & 1 \\ 1 & 1 & -2 \end{bmatrix}.$$

Take the non-linear function $\pounds$ to be

$$\pounds(e_p(\hat{t})) = \begin{bmatrix} -0.5e_{p1}(\hat{t}) + tanh(0.2e_{p1}(\hat{t})) + 0.2e_{p2}(\hat{t}) \\ 0.95e_{p2}(\hat{t}) - tanh(0.75e_{p2}(\hat{t})) \end{bmatrix}.$$

Finding that $\pounds$ meets the condition (2) with

$$S_1 = \begin{bmatrix} -0.5 & 0.2 \\ 0 & 0.95 \end{bmatrix}, \ S_2 = \begin{bmatrix} -0.3 & 0.2 \\ 0 & 0.2 \end{bmatrix}.$$

Pick $\ell = 0.25$, $\rho = 1$, and $\gamma = 1$. For various levels of coupling strength c, the maximum value allowed for sampling period d is listed in Table 1. To show how well the suggested method works, the simulation results are going to be offered. Taking into account $c = 0.5$, $d = 1.8850$, and the other parameters remaining the same, the matrices (all of the derived matrices are unable to be shared here for space concerns) are presented as follows when the Matlab LMI toolbox is applied to acquire workable answers to the linear matrix inequalities in Theorem 1:

$$Z_{01} = \begin{bmatrix} 1.1145 & -0.1685 \\ * & 0.5437 \end{bmatrix}, \ Z_{02} = \begin{bmatrix} 1.1145 & -0.1685 \\ * & 0.5437 \end{bmatrix},$$
$$Z_{03} = \begin{bmatrix} 1.0884 & -0.1648 \\ * & 0.5432 \end{bmatrix},$$
$$Z_{11} = \begin{bmatrix} -2.9011 & 0.3718 \\ * & -1.0621 \end{bmatrix}, \ Z_{12} = \begin{bmatrix} -2.9011 & 0.3718 \\ * & -1.0621 \end{bmatrix},$$
$$Z_{13} = \begin{bmatrix} -2.6249 & 0.3356 \\ * & -1.0571 \end{bmatrix}.$$

Through employing the matrices mentioned above, the following controller gains could be derived with $\daleth = Z_0^{-1} Z_1$:

$$\daleth_1 = \begin{bmatrix} -2.6225 & 0.0401 \\ -0.1289 & -1.9410 \end{bmatrix},$$
$$\daleth_2 = \begin{bmatrix} -2.6225 & 0.0401 \\ -0.1289 & -1.9410 \end{bmatrix}, \quad (34)$$
$$\daleth_3 = \begin{bmatrix} -2.4298 & 0.0143 \\ -0.1193 & -1.9417 \end{bmatrix}.$$

Given the original conditions, $e_1(0) = [-4, 3]^T, e_2(0) = [2, -5]^T, e_3(0) = [3, 1]^T$, as well as $\curlywedge(0) = [-1, 0]^T$, Figs. 1 and 2, respectively, show the trajectory for states in ES (6) and control input $u_p(\hat{t})$ under these controller gains. It can be observed from Figs. 1 and 2 that the control input $u_p(\hat{t})$ satisfies $u_p(\hat{t}) = \daleth_p \hat{e}_p(\hat{t}_f)$, $\hat{t} \in [\hat{t}_f, \hat{t}_{f+1})$. Moreover, it is obvious that FSs (1) and LS (3) are asymptotically synchronous, which illustrates the effectiveness of our approach.

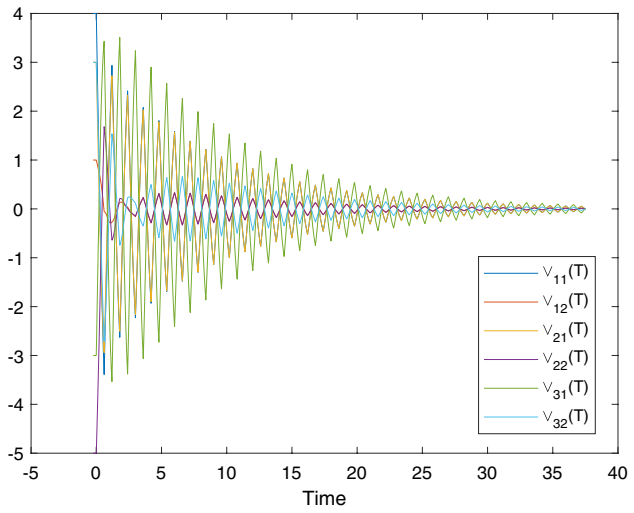

Fig. 1 The state trajectory for error system with control input u(T) of data sampling

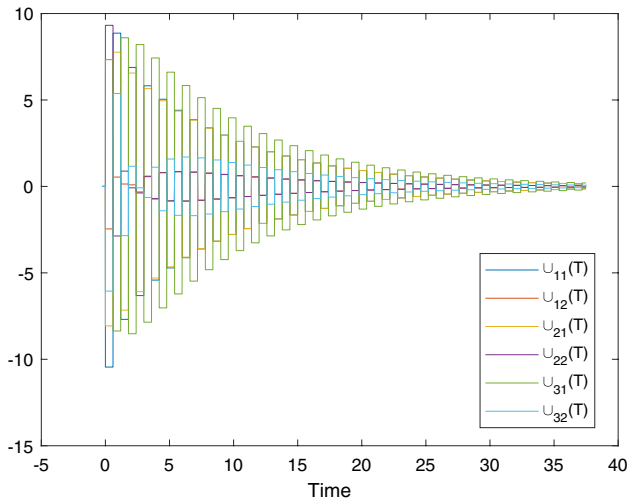

Fig. 2 The control input u(T) of data sampling

Table 1 The highest value allowed for information collection interval d

Refs	[38]	[39]	[40]	Theorem 1
c=0.5	1.3978	1.4979	1.5345	1.8850
c=0.75	1.2619	1.4645	1.4933	1.8880

Example 2 Think about FSs (1) that has three follower systems with the same inner-coupling matrix, outer-coupling matrix, and nonlinear function $\pounds$ as in Example 1.

Take $a = 0.1, \ell = 0.25, \rho = 1$, and $\gamma = 0.5$ as your values. The permissible highest value of the sampling period d is listed under Table 2 for various levels of coupling strength c. The simulation outcomes will be displayed to illustrate the validity of the suggested strategy. Considering $c = 0.8$, $d = 0.4990$, and all other values remaining unchanged, some matrices derived are shown as follows through the use of the Matlab LMI toolbox to achieve workable answers to the linear matrix inequalities in Theorem 2:

Table 2 The highest value allowed for sampling period d with $a = 0.1$

c	0.2	0.4	0.6	0.8
Theorem 2	0.5493	0.5493	0.5490	0.4990

$$R_{01} = \begin{bmatrix} 0.6075 & -0.0818 \\ * & 0.5922 \end{bmatrix}, \quad R_{02} = \begin{bmatrix} 0.6075 & -0.0818 \\ * & 0.5922 \end{bmatrix},$$

$$R_{03} = \begin{bmatrix} 0.3696 & -0.0499 \\ * & 0.5393 \end{bmatrix},$$

$$R_{11} = \begin{bmatrix} -0.4036 & 0.0426 \\ * & -0.7247 \end{bmatrix}, \quad R_{12} = \begin{bmatrix} -0.4036 & 0.0426 \\ * & -0.7247 \end{bmatrix},$$

$$R_{13} = \begin{bmatrix} -0.1959 & 0.0176 \\ * & -0.5100 \end{bmatrix}.$$

Based on the above-given matrices, the following controller gains can be obtained by employing $\daleth = R_0^{-1} R_1$:

$$\daleth_1 = \begin{bmatrix} -0.6671 & -0.0964 \\ -0.0202 & -1.2371 \end{bmatrix},$$

$$\daleth_2 = \begin{bmatrix} -0.6671 & -0.0964 \\ -0.0202 & -1.2371 \end{bmatrix},$$

$$\daleth_3 = \begin{bmatrix} -0.5323 & -0.0811 \\ -0.0166 & -0.9532 \end{bmatrix}.$$

Under these controller gains, the trajectory of states in ES (6) as well as the controlling input $u_p(\hat{t})$, respectively, are presented in Figs. 3 and 4, where $e_1(0) = [8, -9]^T, e_2(0) = [-6, 2]^T, e_3(0) = [6, 4]^T$, and $\curlywedge(0) = [5, 6]^T$. Figs. 3 and 4 show that the control input $u_p(\hat{t})$ meets the condition $u_p(\hat{t}) = \daleth_p \hat{e}_p(\hat{t}_f)$, $\hat{t} \in [\hat{t}_f, \hat{t}_{f+1})$. Additionally, it is clear that FSs (1) and LS (3) are exponentially synchronous, demonstrating the success of our strategy.

6 Conclusions

Emphasize that the main contribution in this article is Lemmas 3 and 5, which can better handle the Lyapunov functional derivative about data sampling systems. Taking advantage of the MFMBIIs, the Lyapunov functional

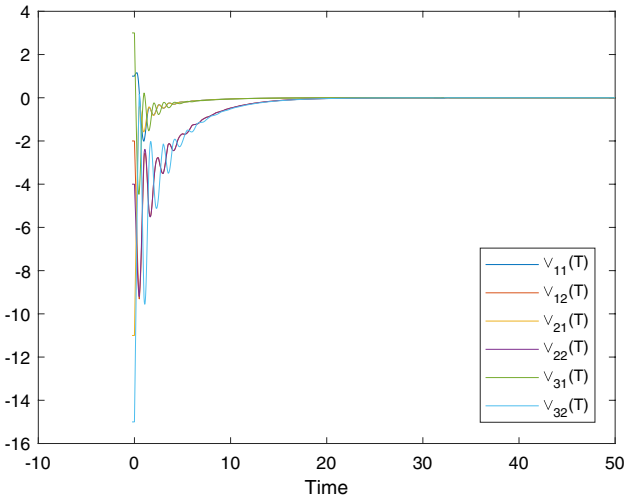

Fig. 3 The state trajectory for error system alongside c=0.8 and a=0.1

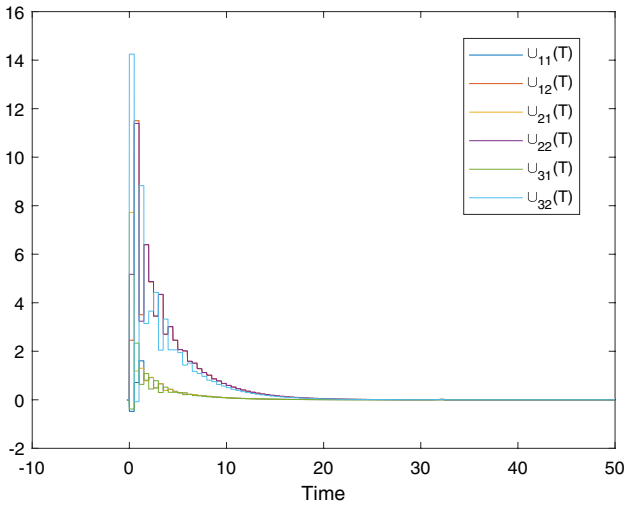

Fig. 4 The data sampling control input alongside c=0.8 and a=0.1

method depending on sampling times, and the convex combination approach, novel standards are developed to make certain that the synchronization error system offers asymptotic and exponential stability, respectively. The effectiveness of new techniques for sampled-data synchronization control is illustrated by two examples. Be aware that many realistic control schemes cannot avoid actuator saturation. Actuator saturation can worsen dynamic behavior or potentially cause the system under investigation to become unstable. In the future, we'll concentrate on the challenge of synchronizing control of delayed and complicated networks with actuator saturation while sampling information. At the same time, new techniques designed for sampling control in this paper will be attempted to extend this topic.

Acknowledgements This research was partially funded by the National Natural Science Foundation of China (6187619 2), the Fundamental Research Funds for the Central Universities (CZT20020), and the Academic Team in Universities (KTZ20051).

Author contributions The authors declare that they have no conflict of interest, and the main manuscript text is written by QZ and reviewed by MJ and JH.

Data availibility Data sharing is not applicable to this article as no datasets were generated or analyzed during the current study.

Declarations

Conflict of interest The authors declare that they have no conflict of interest.

References

1. Wu ZY, Duan JQ, Fu XC (2012) Complex projective synchronization in coupled chaotic complex dynamical systems. Nonlinear Dyn 69:771–779. https://doi.org/10.1007/s11071-011-0303-0
2. Wang JY, Zhang HG, Wang ZS, Wang BR (2013) Local exponential synchronization in complex dynamical networks with time-varying delay and hybrid coupling. Appl Math Comput 225:16–32. https://doi.org/10.1016/j.amc.2013.09.022
3. Wu ZG, Shi P, Su H, Chu J (2013) Sampled-data exponential synchronization of complex dynamical networks with time-varying coupling delay. IEEE Trans Neural Netw Learn Syst 24(8):1177–1187. https://doi.org/10.1109/TNNLS.2013.2253122
4. Liu XH, Xi HS (2014) Synchronization of neutral complex dynamical networks with Markovian switching based on sampled-data controller. Neurocomputing 139(9):163–179. https://doi.org/10.1016/j.neucom.2014.02.048
5. Thendral M, Tamil T, Radhakrishnan G, Babu A, Yang Chandrasekar C (2022) Synchronization of Markovian jump neural networks for sampled data control systems with additive delay components analysis of image encryption technique. Math Method Appl Sci. https://doi.org/10.1002/mma.8774
6. Shen B, Wang ZD, Liu XH (2010) Bounded $H\infty$ synchronization and state estimation for discrete time-varying stochastic complex networks over a finite-horizon. IEEE Trans Neural Netw 22:145–157. https://doi.org/10.1109/tnn.2010.2090669
7. Kaviarasan B, Sakthivel R, Lim Y (2016) Synchronization of complex dynamical networks with uncertain inner coupling

and successive delays based on passivity theory. Neurocomputing 186:127–138. https://doi.org/10.1016/j.neucom.2015.12.071
8. Yang X, Cao J, Lu J (2012) Stochastic synchronization of complex networks with nonidentical nodes via hybrid adaptive and impulsive control. IEEE Trans Circuits Syst 59(2):371–384. https://doi.org/10.1109/tcsi.2011.2163969
9. Chen HB, Shi P, Lim CC (2017) Exponential synchronization for Markovian stochastic coupled neural networks of neutral-type via adaptive feedback control. IEEE Trans Neural Netw Learn Syst 28(7):1618–1632. https://doi.org/10.1109/TNNLS.2016.2546962
10. Wang JL, Wu HN, Huang T, Ren SY (2016) Pinning control strategies for synchronization of linearly coupled neural networks with reaction-diffusion terms. IEEE Trans Neural Netw Learn Syst 27(4):749–761. https://doi.org/10.1109/TNNLS.2015.2423853
11. Wang JY, Zhang HG, Wang ZS, Liu ZW (2017) Sampled-data synchronization of Markovian coupled neural networks with mode delays based on mode-dependent LKF. IEEE Trans Neural Netw Learn Syst 28(11):2626–2637. https://doi.org/10.1109/tnnls.2016.2599263
12. Sakthivel R, Boomipalagan K, Yong MK, Muslim M (2016) Sampled-data reliable stabilization of T-S fuzzy systems and its application. Complexity 21(S2):518–529. https://doi.org/10.1002/cplx.21833
13. Lee SH, Park MJ, Kwona OM, Sakthivel R (2017) Synchronization of Lur'e systems via stochastic reliable sampled-data controller. J Frankl Inst. https://doi.org/10.1016/j.jfranklin.2017.01.003
14. Wu ZG, Park JH, Su HY, Chu J (2012) Discontinuous Lyapunov functional approach to synchronization of time-delay neural networks using sampled-data. Nonlinear Dyn 69:2021–2030. https://doi.org/10.1007/s11071-012-0404-4
15. Yang FS, Zhang HG, Wang YC (2014) An enhanced input-delay approach to sampled-data stabilization of T-S fuzzy systems via mixed convex combination. Nonlinear Dyn 75:501–512. https://doi.org/10.1007/s11071-013-1080-8
16. Li N, Zhang Y, Hu J, Nie Z (2011) Synchronization for general complex dynamical networks with sampled-data. Neurocomputing 74:805–811. https://doi.org/10.1016/j.neucom.2010.11.007
17. Fujioka H (2009) A discrete-time approach to stability analysis of systems with aperiodic sample-and-hold devices. IEEE Trans Autom Control 54(10):2440–2445. https://doi.org/10.1109/tac.2009.2029
18. Kao CY, Fujioka H (2013) On stability of systems with aperiodic sampling devices. IEEE Trans Autom Control 58(8):2085–2090304. https://doi.org/10.1109/tac.2013.2246491
19. Seuret A (2012) A novel stability analysis of linear systems under asynchronous samplings. Automatica 48(1):177–182. https://doi.org/10.1016/j.automatica.2011.09.033
20. Naghshtabrizi P, Hespanha JP, Teel AR (2007) Stability of delay impulsive systems with application to networked control systems, Proc. 26th Am Control Conf 2007:4899–4904. https://doi.org/10.1109/ACC.2007.4282847
21. Briat C (2013) Convex conditions for robust stability analysis and stabilization of linear aperiodic impulsive and sampled-data systems under dwelltime constraints. Automatica 49:3449–3457. https://doi.org/10.1016/j.automatica.2013.08.022
22. Mirkin L (2007) Some remarks on the use of time-varying delay to model sample-and-hold circuits. IEEE Trans Autom Control 52(6):1109–1112. https://doi.org/10.1109/tac.2007.899053
23. Fridman E, Seuret A, Richard JP (2004) Robust sampled-data stabilization of linear systems: an input delay approach. Automatica 40(8):1441–1446. https://doi.org/10.1016/j.automatica.2004.03.003
24. Seuret A, Briat C (2015) Stability analysis of uncertain sampled-data systems with incremental delay using looped-functionals. Automatica 55:274–278. https://doi.org/10.1016/j.automatica.2015.03.015
25. Naghshtabrizi P, Hespanha JP, Teel AR (2008) Exponential stability of impulsive systems with application to uncertain sampled-data systems. Syst Control Lett 57:378–385. https://doi.org/10.1016/j.sysconle.2007.10.009
26. Chen WH, Zheng WX (2012) An improved stabilization method for sampled-data control systems with control packet loss. IEEE Trans Autom Control 57(9):2378–2384. https://doi.org/10.1109/tac.2012.2184629
27. Liu K, Suplin V, Fridman E (2010) Stability of linear systems with general sawtooth delay. IMA J Math Con Inf 27(4):419–436. https://doi.org/10.1093/imamci/dnq023
28. Liu K, Fridman E (2012) Wirtinger's inequality and Lyapunov-based sampled-data stabilization. Automatica 48(1):102–108. https://doi.org/10.1016/j.automatica.2011.09.029
29. Chandrasekar A, Radhika T, Zhu Q (2022) State estimation for genetic regulatory networks with two delay components by using second-order reciprocally ConVex approach. Neural Process Lett 54:327–345. https://doi.org/10.1007/S11063-021-10633-4
30. Fridman E (2010) A refined input delay approach to sampled-data control. Automatica 46(2):421–427. https://doi.org/10.1016/j.automatica.2009.11.017
31. Wu ZG, Shi P, Su HY, Chu J (2012) Exponential synchronization of neural networks with discrete and distributed delays under time-varying sampling. IEEE Trans Neural Netw Learning Sys 23:1368–1376. https://doi.org/10.1109/TNNLS.2012.2202687
32. Zhang C, He Y, Wu M (2010) Exponential synchronization of neural networks with time-varying mixed delays and sampled-data. Neurocomputing 74:265–273. https://doi.org/10.1016/j.neucom.2010.03.020
33. Zeng HB, He Y, Wu M, She JH (2015) Free-matrix-based integral inequality for stability analysis of systems with time-varying delay. IEEE Trans Automatic Control 60:2768–2772. https://doi.org/10.1109/tac.2015.2404271
34. Zeng HB, He Y, Wu M, She JH (2015) New results on stability analysis for systems with discrete distributed delay. Automatica 60:189–192. https://doi.org/10.1016/j.automatica.2015.07.017
35. Zeng HB, Park JH, Xiao SP, Liu Y (2015) Further results on sampled-data control for master-slave synchronization of chaotic Lur'e systems with time delay. Nonlinear Dyn 82:851–863. https://doi.org/10.1007/s11071-015-2199-6
36. Lee TH, Park JH (2017) Stability analysis of sampled-data systems via free-matrix-based time-dependent discontinuous lyapunov approach. IEEE Trans Automatic Control 62(7):3653–3657. https://doi.org/10.1109/tac.2017.2670786
37. Gunasekaran N, Zhai GS, Yu Q (2020) Sampled-data synchronization of delayed multi-agent networks and its application to coupled circuit. Neurocomputing 413:499–511. https://doi.org/10.1016/j.neucom.2020.05.060
38. Chen Z, Shi KB, Zhong SM (2016) New synchronization criteria for complex delayed dynamical networks with sampled-data feedback control. ISA Trans 63:154–169. https://doi.org/10.1016/j.isatra.2016.03.018
39. Lee SH, Park MJ, Kwon OM, Sakthivel R (2017) Advanced sampled-data synchronization control for complex dynamical

networks with coupling time-varying delays. Inf Sci 420:454–465. https://doi.org/10.1016/j.ins.2017.08.071
40. Wang X, Liu XZ, She K, Zhong SM, Zhong QS (2019) Extended dissipative memory sampled-data synchronization control of complex networks with communication delays. Neurocomputing 347:1–12. https://doi.org/10.1016/j.neucom.2018.10.073
41. Liu PL (2015) New results on delay-range-dependent stability analysis for interval time-varying delay systems with non-linear perturbations. ISA Trans 57:93–100. https://doi.org/10.1016/j.isatra.2015.03.001